University of Stuttgart

Institute of Geodesy

Analysis of Long Term Variations of Ocean Mass in the Arctic Region using Satellite Gravimetry

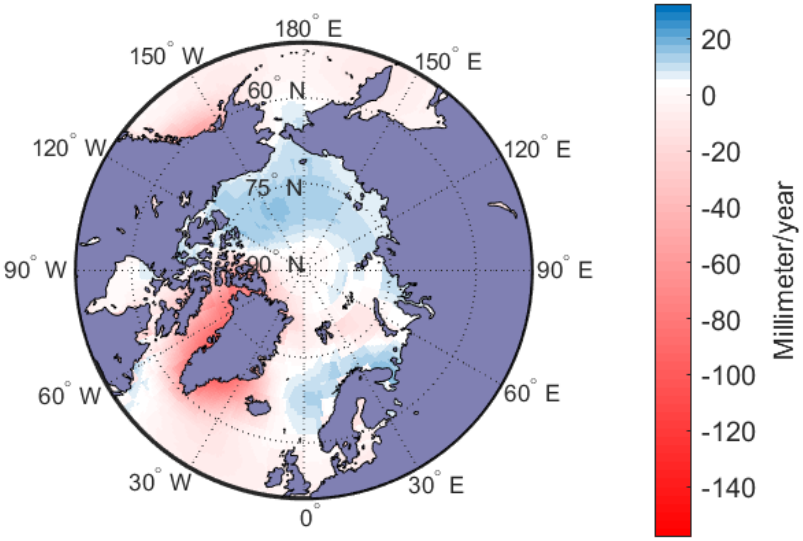

Master Thesis

Geomatics Engineering

University of Stuttgart

Thomas Daud Gisiri

Stuttgart, December 2020

Supervisor: **Dr. –Ing. Mohammad J. Tourian**
Prof. Dr. –Ing. Nico Sneeuw

University of Stuttgart

Declaration

I declare that this thesis has been composed solely by myself and that it has not been submitted, in the whole or in part, in any previous application for degree. Except where stated otherwise by references or acknowledgement, the work presented is entire my own.

…… ……..……

Place, Date Signature

Abstract

The Arctic region has experienced rapid sea ice melt in the past decade, which leads to the global sea level rise. The volume of the ice, area and extent have been declining in recent years. The inflow of the Atlantic Ocean water into Arctic Ocean have made changes including the weaker stratification. Moreover, shoaling of Atlantic water in Eurasian Basin reduced sea ice and accelerate the Atlantic water layers' heat fluxes further Northeast into Eurasian Basin. The salty water (denser than fresh water), the melting of sea ice and warming of Arctic Ocean surface are causing the density of water to change as well as the variations in ocean mass. These huge amounts of the mass variations lead the variations of the Earth gravity field that are being monitored by satellite gravimetry. The main objective of this thesis is to estimate and analyse ocean mass variations in the Arctic Ocean and all seas around namely Laptev Sea, Kara Sea, Barents Sea, Green Land Sea, Baffin Bay, Hudson Bay, Baffin Bay, Beaufort Sea, Chukchi Sea and East Siberian Sea. For this purpose, the standard GRACE level-2 data product from GeoForschungsZentrum (GFZ), Potsdam and the Centre for Space Research (CSR) from University of Texas has been used to estimate the ocean masses. Moreover, the Sea Level Anomaly (SLA) data from satellite altimetry was used for further analysis of the trend in the Arctic region computed from GRACE data. The SLA data is provided by Technical University of Denmark (DTU). Results show that the Beaufort Sea has experienced the highest positive trend in ocean mass of 9.99 mm/year and SLA of approximately 10 mm/year. The positive trends are influenced by the presence of Beaufort Gyre which the anticyclone winds accumulate the fresh water and deeper in this region there are cold and salty water from Pacific Ocean. The Chukchi Sea has positive trend in ocean mass of 7.64 mm/year and Sea Level Anomaly trend range from -1 mm/year and 1 mm/year. The positive trends are influenced by Pacific Ocean water which are warmer and saltier. The Baffin Bay has the strongest negative trend in ocean mass of -59.59 mm/year and Sea Level anomaly trend of approximately -9 mm/year. These negative trends are caused by the Gravitation attraction of Greenland masses and the Arctic ocean freshwater outflows through it on the way to North Atlantic Ocean. The Hudson Bay have positive trend in ocean mass of 0.35 mm/year and Sea Level Anomaly trend ranges from 1 to 3 mm/year. The positive trends are due to large input of fresh water from river and precipitation, ice melting influenced by air temperature and inflow of Arctic Ocean waters. The Greenland Sea has negative trend in ocean mass of -9.10 mm/year and Sea Level Anomaly trend ranges between -1 mm/year and 6 mm/year. The negative trend is influenced by Gravitational attraction of Greenland masses or due to freshwater outflow from the Arctic ocean through western side of Fram Strait. Barents Sea has positive trend in ocean mass of 0.13 mm/year and Sea Level Anomaly trend ranging from -1 mm/year to 7 mm/year. Kara sea has positive trend in ocean mass of 3.73 mm/year, Laptev sea has positive trend in ocean mass of 6.83 mm/year, East Siberian Sea has a positive trend of 8.25 mm/year and Arctic ocean has positive ocean mass trend of 5.83 mm/year. The positive trends in this region are influenced by the so-called Atlantification of Arctic ocean. The Kara Sea, Laptev Sea and East Siberian Sea all have negative trends in Sea Level Anomaly ranging from -2 mm/year to -6 mm/year. The negative trends are influenced by the gain of fresh water, net precipitation, run off increased and more discharge from the land to the sea water.

Key words: Satellites gravimetry; Ocean mass; Arctic region; Sea Level Anomaly

Acknowledgement

This thesis would not have reached a successful destination without support, help and encouragement of many individual appreciations. I thank almighty God, the creator and overseer, who gave me the strength and wisdom for achieving this important analysis.

I would like to express my genuine appreciation to the Government of United Republic of Tanzania through the Ministry of Lands, Housing and Human Settlement Developments and Department of Land Surveys and Mapping for offering me the Scholarship to pursue Master of Science in Geomatics Engineering at the University of Stuttgart, Germany.

Deep appreciation should directly go to my supervisors Dr. – Ing. Mohammad J. Tourian and Prof. Dr.–Ing. Nico Sneeuw for their strongest supervision, constant tirelessly and overestimated support, technical and timely guidance, encouragement, valuable advice, and suggestions from the beginning to the end of this thesis.

My sincere thanks should go to my fellow students, Institute of Geodesy staff members and all individuals whom in one way or another helped me to complete this thesis.

Furthermore, I wish to express my gratitude to my daughter Noela, my Parents Mr. Mwita Gisiri and Mrs. Mariam J. Marunguri, my brothers and sisters and all relatives. I really appreciate their love, serenity, and strong encouragement during hard time of being far away from them. These may be material things and/or non-material such as prayers which help me to grow physically, mentally, and spiritually.

Table of Contents

List of Figures

List of Tables

List of Abbreviations and Acronyms

AOD1B	Atmosphere and Ocean 1B De aliasing
CSR	Centre for Space and Research
DLR	Deutsches Zentrum fur Luft- und Raumfahrt
DTU	Technical University of Denmark
ECMWF	European Centre for Medium – Range Weather Forecasts
Envisat	Environmental satellite
ERS	European Remote Sensing Satellite
ESA	European Space Agency
ESSP	Earth System Science Pathfinder
EWH	Equivalent Water Height
GFZ	GeoForschungsZentrum
GIA	Glacial Isostatic Adjustment
GPCP	Global Precipitation Climatology Project
GPS	Global positioning system
GRACE-(FO)	Gravity Recovery And Climate Experiment (Follow On)
GSOC	Germany Space Operations Centre
IHO	International Hydrographic Organisation
IMU	Inertial Measurement Unit
ISDC	Information System and Data Science
JPL	Jet Propulsion Laboratory
LAGEOS-1	LAser GEOdynamics Satellite-1
LRI	Laser Ranging Interferometer
MIB	Modified Inverse Barometer
MSSH	Mean Sea Surface Height
NASA	National Aeronautics and Space Administration
NWP	Numerical Weather forecast Prediction
OBP	Ocean Bottom Pressure

PODAAC	Physical Oceanography Distributed Active Centre
SLA	Sea Level Anomaly
SSH	Sea Surface Height
SST	Sea Surface Temperature
UTCSR	University of Texas Centre for Space and Research

Chapter 1

Introduction

1.1 Motivation

In the past decade, the Arctic region has experienced rapid sea ice melt, which contributes to the global sea level rise that is one of the climate change indicators. The volume of the ice, area and extent have been declining in recent years. These changes cause the loss of reflectivity or Albedo of the sea ice, leading to the fact that most of sun's radiation are absorbed by dark ocean water that leads to more melting and warming in Arctic region. Meanwhile, the warm temperature greater than 0^0C and salty water from Northern part of Atlantic Ocean spread throughout the deep basins at intermediate depth (approximately 150 to 900m) and hold the sufficient heat to melt the Arctic sea ice (Polyakov, I. V., et al, 2020).

The inflow of the Atlantic Ocean water into Arctic Ocean have made changes including the weaker stratification and shoaling of Atlantic water in Eurasian Basin, which at the same time reduced sea ice and accelerate the Atlantic water layers' heat fluxes. This process is referred to as "Atlantification" of Arctic Ocean (Polyakov, I. V, et al, 2017; Timmermans and Marshall, 2020). The salty water (denser than fresh water), the melting of sea ice and warming of Arctic Ocean surface are causing the density of water to change as well as the variations in Ocean mass. These huge amounts of the mass variations lead to a change in the variations of the Earth gravity field that is sensed by Satellite Gravimetry (Yi, S. 2019). The studying and analysing of mass variations in the entire Arctic region using Satellite Gravimetry will help the understanding of the Arctic dynamic sea level changes.

The GRACE (Gravity Recovery and Climate Experiment) was the joint mission between the National Aeronautics and Space Administration (NASA) and the German Aerospace Centres (DLR). For the period of more than 15 years, the GRACE mission has monitored the mass changes of water cycle in the Earth every month from year 2002 to 2017. Since June 2018, GRACE Follow On (GRACE-FO) continues with monitoring the earth's water movement, sea level caused by addition of water in the Ocean, soil moisture, amount of water in large lakes and rivers, underground water storage as well as ice sheets and glaciers (Landerer et al., 2020).

The main objective of this thesis is to estimate and analyse ocean mass variations in the Arctic Ocean and all seas around it including Laptev Sea, Kara Sea, Barents Sea, Green Land Sea, Baffin Bay, Hudson Bay, Baffin Bay, Beaufort Sea, Chukchi Sea and East Siberian Sea. For this purpose, the standard level-2 (spherical harmonic coefficients) GRACE data product from GeoForschungsZentrum (GFZ), Potsdam and the Centre for Space Research (CSR) from University of Texas have been used to estimate the ocean masses.

Moreover, the Sea Level Anomaly (SLA) data from satellite altimetry was used for further analysis of the trend in the Arctic region computed from GRACE data. The SLA data is provided by Technical University of Denmark (DTU). For the comparison purposes only the SLA data with the same period of GRACE data (2002 to 2017) was used to compute a trend map. Similarly, the Global Precipitation Climatology Project (GPCP) data includes the observations from Satellites and gauge stations to estimate the monthly rainfall on the global grid of 2.5^0 by 2.5^0 latitude and longitude from 1979 to present (Adler et al. 2003). Precipitation trend over the ocean was computed and has a complete analysis of rainfall available over entire Arctic region.

1.2 Background of GRACE mission

In 1996 the GRACE mission was proposed cooperatively by the three organisations, University of Texas of Austin, The German research for sciences (GFZ) and the Jet Propulsion Laboratory (JPL) in Pasadena (GFZ, 2020). In May 1997, the GRACE mission was selected as a second mission under the NASA Earth System Science Pathfinder (ESSP) Program (UTCSR, 2020). Professor Byron Tapley from University of Texas Centre for Space and Research (UTSCR) was the principal investigator of the mission and his team were the key investigators for developing a flight mission hardware from selection to launching of satellite and the Co-principal investigator of this mission was Dr. Frank Flechtner from GFZ and the JPL was responsible for the project management and system engineering (GFZ, 2020).

The GRACE mission was jointly implemented by National Aeronautics and Space Administration (NASA) and the German Aerospace Centres (DLR), successfully Launched on March 17, 2002 with the main objective of accurate estimation of the Earth gravity field and its variation over time (Tapley et al., 2004). The design lifetime of the GRACE mission was 5 years but for 15 years, GRACE mission has been recording the change of the mass of the Earth and the mission ended in June 2017 (Landerer et al., 2020).

1.2.1 How does GRACE monitor time variable gravity field?

The twin satellite as shown in Figure 1.1 was near polar and circular orbit with an Inclination of $89^0$and at an altitude of approximately 500 km. The GRACE mission concept is based on low-to-low satellite tracking, where the two satellites follow each other in the same orbit around the Earth and separated at distance approximately by 220 km (Yi, S. 2019). The twin satellite carries dual frequency K-band Microwave Ranging (KBR) system to continuous monitoring the changes which later imply the changing of gravity of the Earth. The satellites carry high precise accelerometers located in the centre of gravity of each satellite for measuring non-gravitational attraction such as atmospheric drag, solar radiations, and Earth Albedo. The Global Positioning System (GPS) receivers to determine the absolute positions of the satellites over the Earth and derivations of distances between the satellites and attitude sensors (Tapley et al., 2004).

The variations in Earth's gravity field caused the change in distances between the two satellite in the orbit, where the area with higher mass concentration (stronger gravity) will attract the lead satellite and accelerate it away from the following satellite. As the pair continue orbiting the Earth,

the following satellite also is attracted by area of higher mass concentration towards the lead satellite. The distance changes between satellites are measured by high accurate dual frequency K-band Microwave Ranging (KBR) system. The observed distances are corrected for non-gravitational attractions effects by very precise accelerometers that measure the surface force accelerations. The GPS receivers of each satellite measure the absolute positions of the satellites over the Earth and the derivations of distance changes between the satellite and the attitude sensors were used to obtain very precise inertial orientation of the GRACE satellites (Seeber G., 2003; Tapley et al., 2004).

All these data are gathered and used to create the monthly global gravity field of the Earth and offered the information on changes in distribution of masses over the land and oceans (Seeber G., 2003).

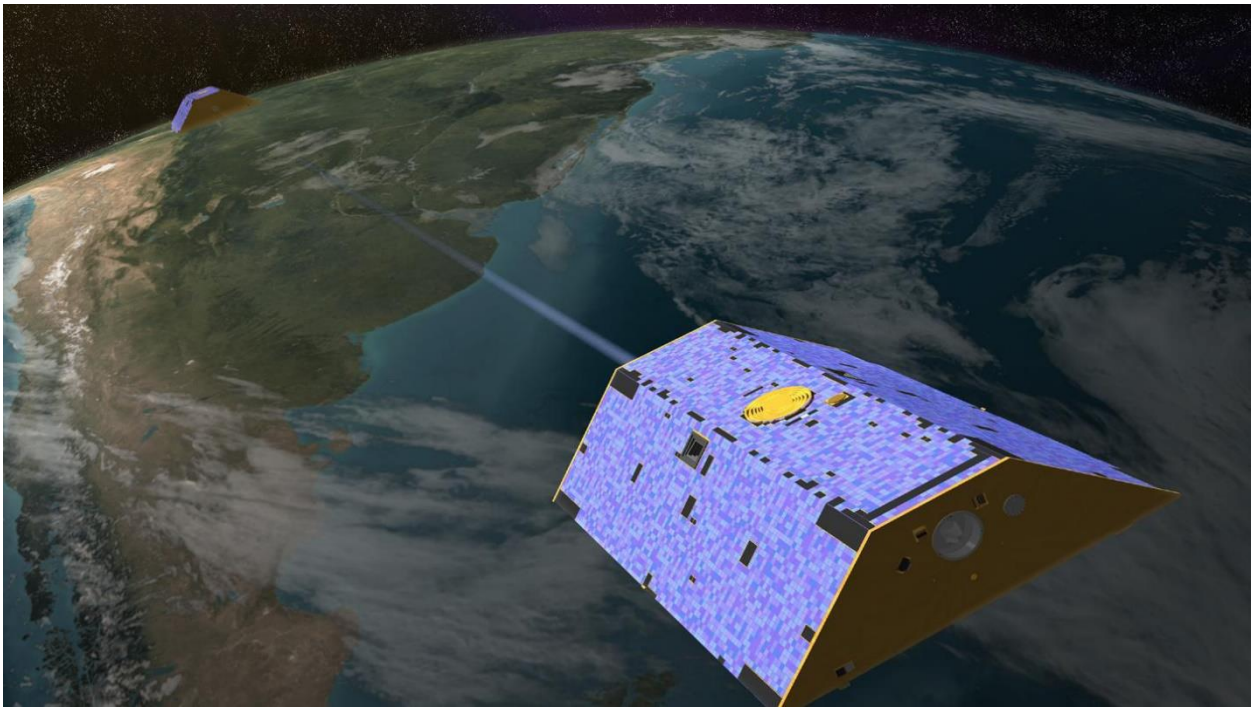

Figure 1.1: Illustration of the twin GRACE satellites in orbit (Credit: NASA/JPL-Caltech)

1.3 The GRACE-FO mission

The Gravity Recovery and Climate Experiment Follow On (GRACE-FO) mission is the successor of previous GRACE mission (2002-2017). It was launched successfully on 22 May 2018. The GRACE-FO is the collaboration between NASA and GFZ with the main objective of continuing with the original purposes of GRACE mission (GFZ, 2020). The primary objective of GRACE-FO is continuing providing the global measurements of monthly gravity field models of the Earth. For this purpose, the GRACE-FO adopts the measurements principles of GRACE as described in section 1.2.1 with GPS receiver in each satellite, K- and Ka- band Microwave Ranging System,

Precise Accelerometer, Attitude sensors with three Star Cameras and Angular rate sensing Inertial Measurement Unit (IMU) (GFZ, 2020; Landerer et al., 2020).

A secondary objective of the GRACE-FO is the demonstration of new technology of Laser Ranging Interferometer (LRI). This is the satellite-to-satellite laser ranging as microwave ranging system with much higher accuracy and the future technology for GRACE - like missions (GFZ, 2020; Landerer et al., 2020).

1.3.1 GRACE- FO Data Processing System

The GRACE-FO ground segment is identical to that of the GRACE as illustrated in Figure 1.2 below. Where the GFZ satellite receiving station located at Ny-Ålesund, Spitsbergen in Norway and the Germany Space Operations Centre (GSOC) of the DLR which has two ground stations in Weilheim and Neustrelitz in Germany. These stations are responsible for real time monitoring of GRACE-FO satellite status during satellites overflights and they are responsible for the science data downlinks and housekeeping (Landerer et al., 2020). The received data is then transmitted to the DLR's Raw Data Centre (RDC) in Neustrelitz in Germany and distribute them to the Information System and Data Centre (ISDC) at GFZ, UTCSR and Physical Oceanography Distributed Active Centre (PODAAC) at JPL (Landerer et al., 2020).

Since the GRACE era, the GRACE Science Data System (SDS) proceeding with producing the monthly global gravity field of the Earth from the three processing centres (GFZ, JPL and UTCSR) (Cooley, S. and Landerer, F., 2019). Also, the GRACE-FO data is distributed in these processing centres in three levels derived from GRACE satellite observations:

- Level 1 processing: The level 0 is the raw data from the satellites and instrument telemetry. The Level 1A products consist of time tagged and their sampling rate are reducing to get Level 1B. the level 1B products consist of the K/Ka-band microwaves links and Laser Ranging interferometer measurements and the GPS, Accelerometer, and star cameras observations (GFZ, 2020; Landerer et al., 2020).
- Level 2 processing: at this stage, the monthly average of gravity models in terms of spherical harmonic coefficients of the gravitational potential of the Earth is estimated up to degree and order of 60 by 60 and 96 by 96. The SDS also produce the Atmosphere and Ocean 1B De aliasing (AOD1B) background models to restore the corresponding atmospheric and ocean signals which were removed during Level 1 processing (Landerer et al., 2020; GFZ, 2020; Dobslaw et al., 2017).
- Level 3 processing: are produced from converting the GRACE level 2 spherical harmonic coefficients to the gridded geopotential functional, for example equivalent water thickness (GFZ, 2020). The conversions of GRACE level 2 require various steps including removal of correlated and random errors, restoring background models and corrections of glacial isostatic adjustments (GIA) (Cooley, S. and Landerer, F., 2019).

In this study, the standard GRACE level 2 data have been used to estimate the long-term variations of Ocean mass in the Arctic region.

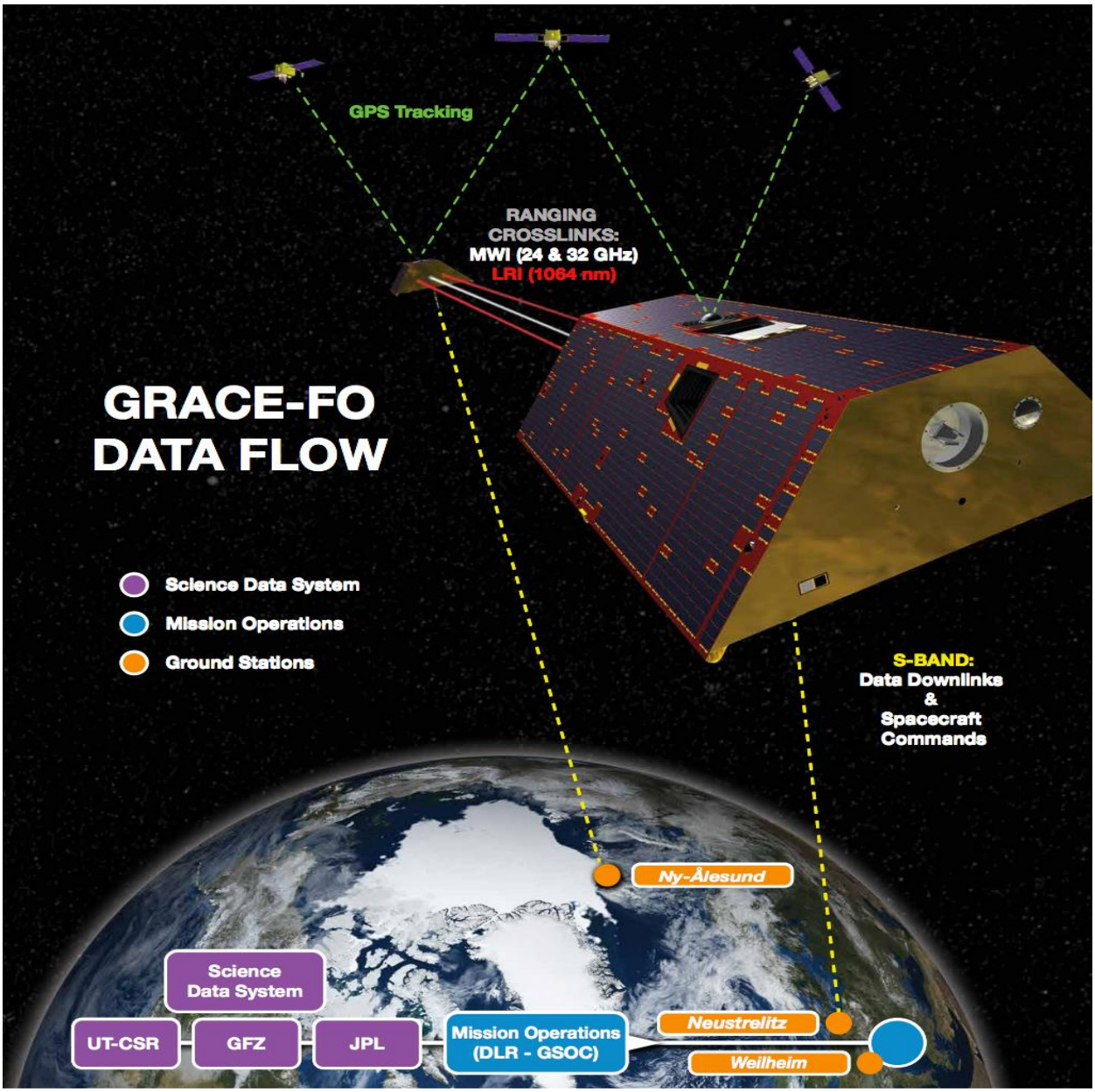

Figure 1.2: The GRACE and GRACE-FO mission Science Data System and Flow (Credit: Cooley, S. and Landerer, F. 2019).

1.4 Study area

The study area is the Arctic region with different basins shown in Figure 1.1 which are Arctic Ocean, Laptev Sea, Kara Sea, Barents Sea, Green Land Sea, Baffin Bay, Hudson Bay, Baffin Bay, Beaufort Sea, Chukchi Sea and East Siberian Sea. Table 1.1 summarized the basins division

information and area of each basin. The source for the boundaries is the publication 'Limits of Oceans and Seas' Special Publication No. 23 published by IHO in 1953 (Flanders Marine Institute, 2018).

Table 1.1: The basin division basic information

S/N	Basins	Coordinates (Latitude, Longitude)	Area (km^2)
1	Laptev Sea	75.4937^0N, 122.0066^0E	513,667
2	Kara Sea	75.4299^0N, 77.3924^0E	896,938
3	Barents Sea	74.7239^0N, 42.1178^0E	1,408,430
4	Greenland Sea	74.7239^0N, 8.3032^0W	1,186,456
5	Baffin Bay	74.5061^0N, 67.1217^0W	529,960
6	Hudson Bay	59.0359^0N, 84.8891^0W	832,649
7	Beaufort Sea	72.1392^0N, 136.8292^0W	431,132
8	Chukchi Sea	72.1392^0N, 156.9730^0W	346,259
9	East Siberian Sea	69.4799^0N, 159.3441^0E	633,067
10	Arctic Ocean	84.8649^0N, 5.2026^0W	5,120,993

Source: https://upload.wikimedia.org/wikipedia/commons/9/98/Political_Map_of_the_Arctic.pdf

Figure 1.3: The Map of Arctic region showing the study area

1.5 Organisation of the thesis

This thesis is organized into five chapters. Chapter 1 comprises of introduction, background of GRACE mission and study area. Chapter 2 describes the overview of ocean water. Chapter three describes the data used to achieve the objective of this thesis. In Chapter 4, the data processing and computation are discussed. Chapter 5 comprises the results obtained from GRACE data processing, Sea Level Anomaly from Altimetry and Precipitation data. Chapter 6 comprises the analysis and discussion of the results from GRACE data processing, Sea Level Anomaly from Altimetry and Precipitation data. Chapter 7 concludes this study based on the results obtained.

Chapter 2

Ocean Water

Since we are dealing with variations of mass in ocean water, this chapter describe the physical properties of ocean water. In the following, the effect of salt in the ocean water is discussed, the overview of the how ocean water reacts to the increase or decrease in temperature is given, and a discussion on how ocean salinity and temperature affect the density of the sea water is provided.

2.1 Salinity of the ocean water

Salinity is the total amount of dissolved material in grams in one kilograms of the sea water expressed in part per thousand or practical salinity unit. The distribution of salinity and temperature is controlled by evaporation and precipitation as well as ice melt and river discharge. The changes in temperature and salinity result to the changes in the density of sea water surfaces, which can lead to convection and changes in the deeper ocean circulation (Stewart R.H. 2000).

The sea surface salinity as shown in Figure 2.1 is high at mid-latitudes where the evaporation is high, and less salinity are found near the equator where the rainfall freshens the surface water and at high latitudes (poles) where ice melting freshens the water. The salt has effect on the sea water; it makes the sea water denser than fresh water. Typically, the salinity of sea water ranges between 33-37 gram of salt per litre of water or practical salinity unity (Stewart R.H. 2000).

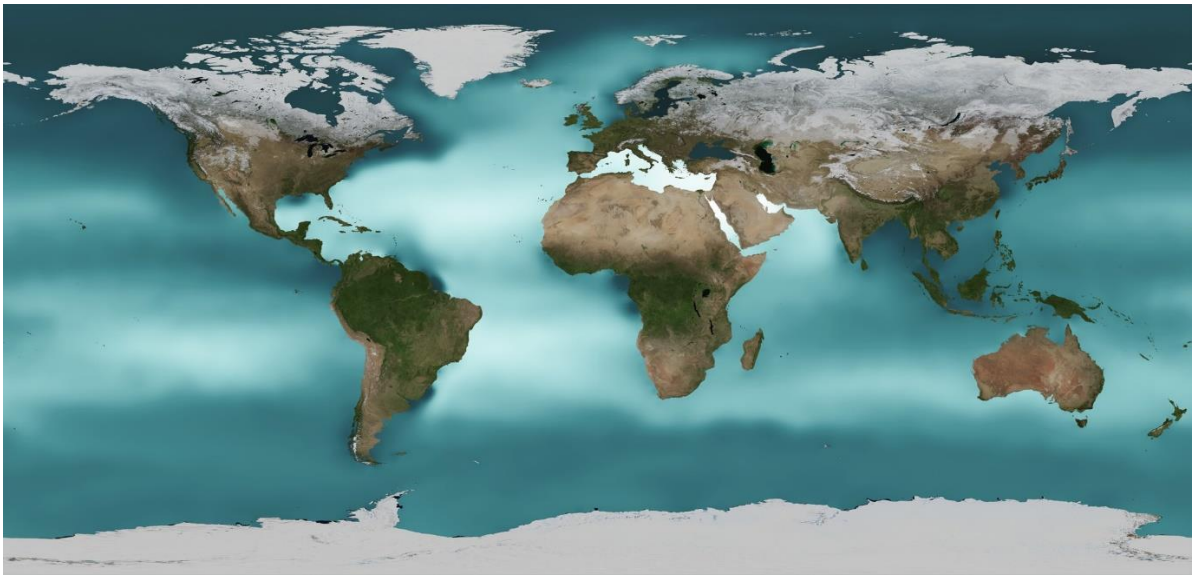

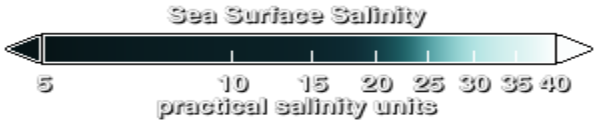

Source (https://svs.gsfc.nasa.gov/3652)

Figure 2.1: The Global map of average Sea Surface Salinity (SSS)

2.2 Temperature of ocean water

The distribution of temperature at the sea surface is independent of longitude in fact that the warm water is at equator and cold water is near the poles as shown in Figure 2.2. Temperature changes over the sea water has an impact on density of sea water in fact that when the water warms it expands and become less dense. In this aspect the warm sea water is less dense than cold sea water (Stewart R.H. 2000).

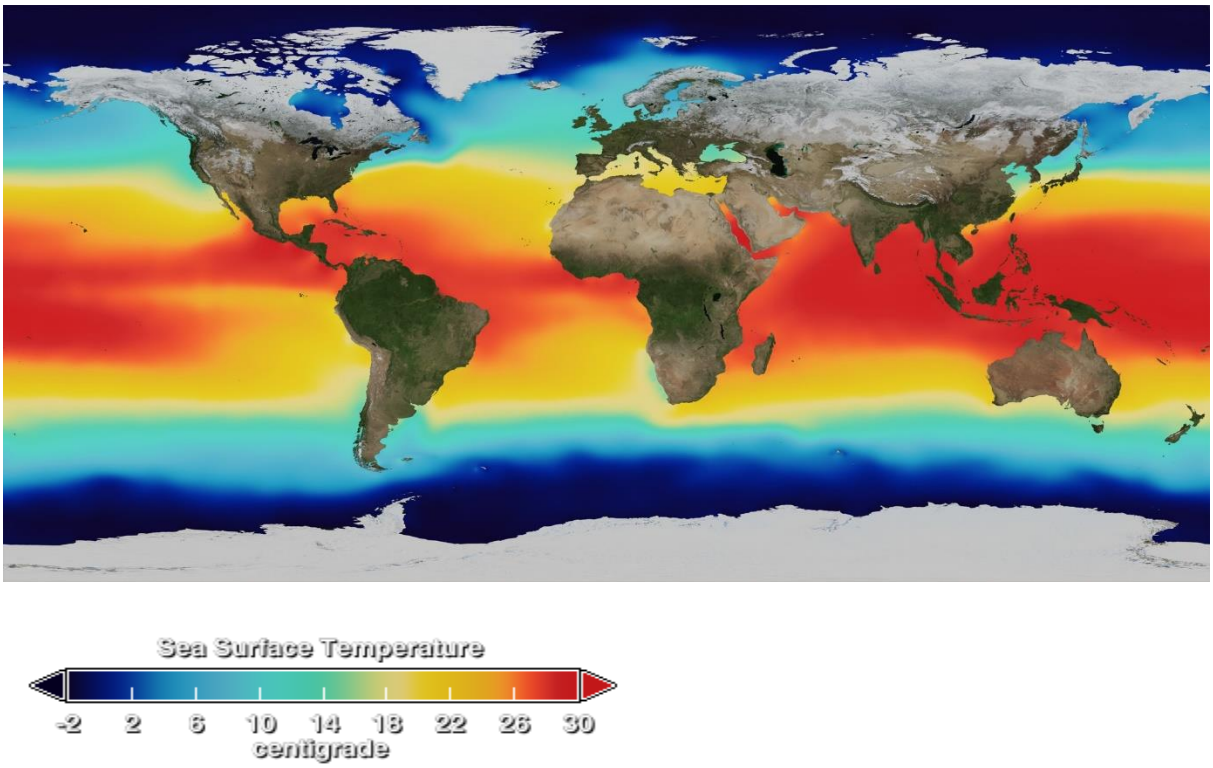

Source (https://svs.gsfc.nasa.gov/3652)

Figure 2.2: The Global map of average Sea Surface Temperature (SST).

2.3 Density of ocean water

The density of ocean water is calculated from the measurement of temperature, conductivity or salinity and pressure using the equation of state of the sea water. The density of pure water is $1000kg/m^3$ at the surface of the ocean the is $1027kg/m^3$ because of the salinity in it the sea water is denser than pure water. This imply that if the sea water has high salinity means its density also increases too as well as the mass in it increases (Stewart R.H. 2000).

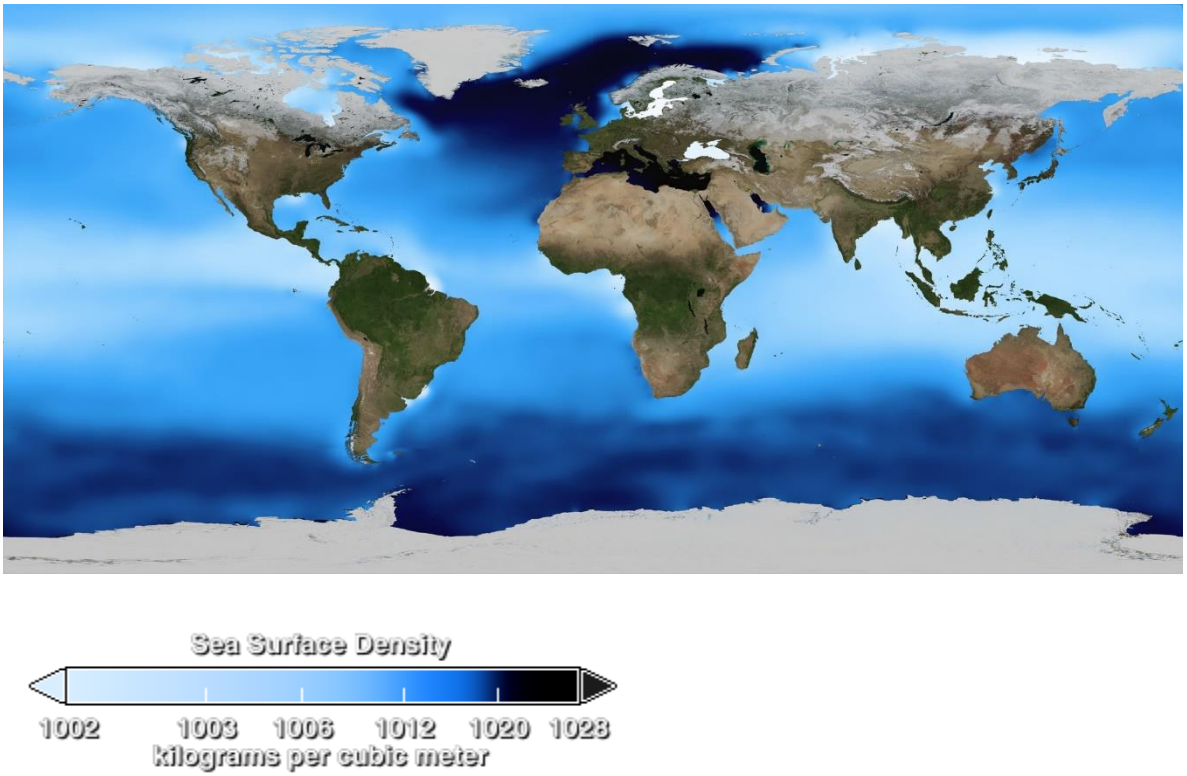

Source (https://svs.gsfc.nasa.gov/3652)

Figure 2.3: The Global map of average Sea Surface Density.

2.4 Surface mixed layer of the ocean water

The ocean water is mixed in the upper layer by the wind blowing and waves lead to surface mixed layer. The surface mixed layer is the thin layer of the surface of the sea water having a constant temperature and salinity from the surface down to depth where the values change from those of the surface. The mixed layer is approximately 10 to 200 m thick over the tropical and mid-latitude belts (Stewart R.H. 2000).

Below the surface mixed layer as shown in Figure 2.4 the temperature falls rapidly with the increase in depth. This layer in which depth increases with decrease in temperature gradient is known as *Thermocline*. The density, salinity and temperature of sea water are closely related, the layer at which the density increases rapidly with increase in depth is called *Pycnocline* and the layer at which salinity increase with increase in depth is called *Halocline* (Stewart R.H. 2000).

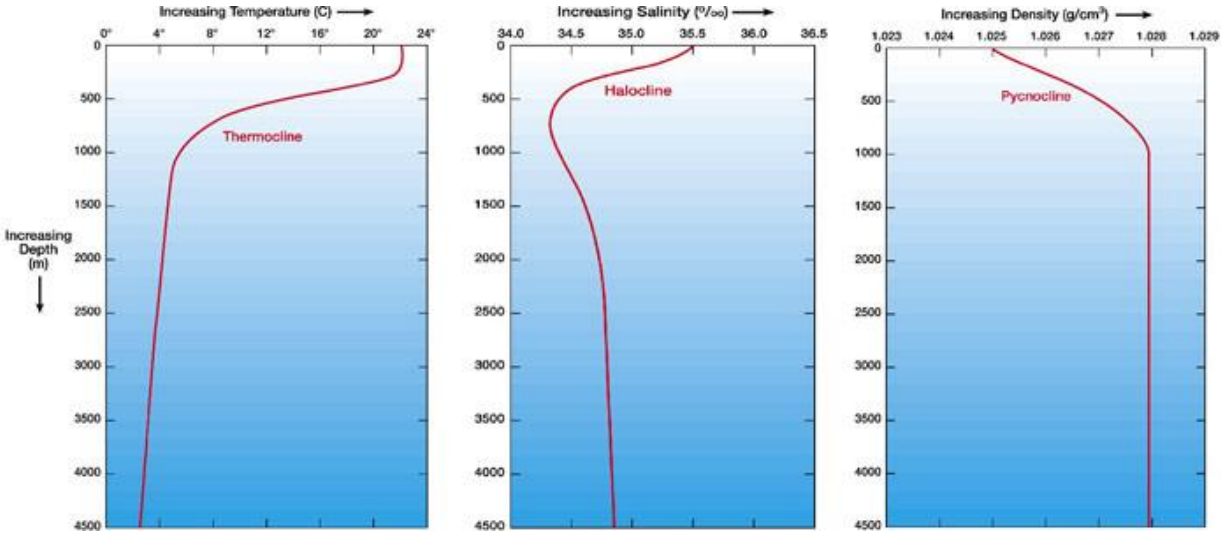

(Source: http://www.hurricanescience.org/science/basic/water/)

Figure 2.4: The properties of water in open ocean with respect to salinity, temperature, and density

In Arctic region the relatively cold, fresh water lie on top of relatively warm salty water as shown in Figure 2.5 and separated by strong halocline. In contrast in the subtropical oceans the stratification is set by temperature where the warmer waters overlay the cold waters. Both Canadian Basin and Eurasian basin warm Atlantic origin resides between depth of approximately 50 to 500 m with temperature range from 0 to 3^0C (Timmermans and Marshall, 2020).

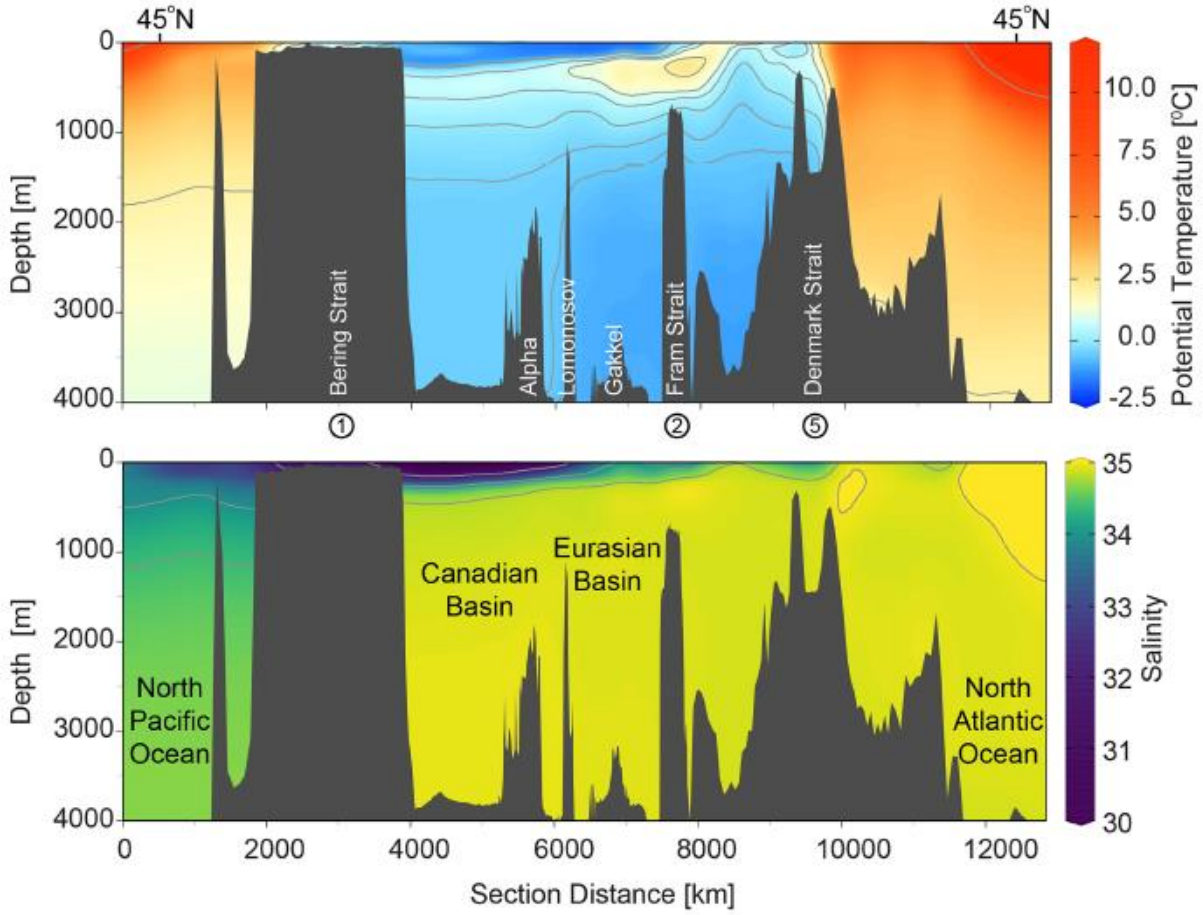

Figure 2.5: The sections of Potential temperature (^{0}C) (Top) and Salinity (bottom) from the Chukchi sea to the Eurasian Basin (Credit: Timmermans and Marshall, 2020)

Chapter 3

Data

This chapter will describe all data used in this thesis. As explained in chapter one in the motivation section, we are dealing with analysis of the long-term ocean mass variation in Arctic region using Satellite Gravimetry. In this chapter the GRACE level-2 data and restoring of the AOD1B background models are described, all standard correction to GRACE data like replacing degree 2 of GRACE data with degree 2 of Satellite Laser Ranging and adding degree 1 coefficients to GRACE data. The Sea Level Anomaly (SLA) data from Satellite Altimetry are discussed here and the Precipitation data are explained in this chapter. Finally, the boundary information data of the Arctic ocean and all seas around it are discussed.

3.1 GRACE data

The GRACE level-2 (gravity models in terms of spherical harmonic coefficients of the external gravitational potential of the Earth) data Release 06 were used to calculate the Equivalent Water Height (EWH) over the land and Ocean mass. The GRACE level-2 data are produced by three centres as part of GRACE ground system which are GeoForschungsZentrum (GFZ), Potsdam, the Centre for Space Research (CSR) from University of Texas and Jet Propulsion Laboratory (JPL) (Landerer et al., 2020). In this study the data from GeoForschungsZentrum (GFZ), Potsdam and the Centre for Space Research (CSR) from University of Texas have been used.

During GRACE level-1 processing, the effects of ocean and atmosphere redistributions are removed prior to accumulating and solving monthly normal equations. For the ocean analysis using GRACE level-2, this Atmosphere and Ocean 1B De aliasing (AOD1B) background models must be restored back before further analysis. These models are very important because they help to convert the GRACE level-2 products into mass driven sea level change for the comparison with the sea level change produced by radar altimetry (Uebbing, B. et al., 2019).

The individual processing centres reduce the modelled atmosphere and ocean mass distribution with the temporal resolution of 3 hours for Release 06. These processing centres provide various products: (1) the GRACE level-2 data is provided with respect to these products here denoted as GSM (represent the full magnitude of land hydrology, ice, and solid Earth process), (2) the GAC products represent Global atmospheric and Ocean signal of the background models and (3) the GAD products (defined only over the ocean) are used to add ocean bottom pressure of the background models and dis-regarding the upper air density anomalies. (Swenson et al., 2008; Uebbing, B. et al., 2019)

Since we are dealing with ocean mass variation, the GAD product must be added to original GRACE level-2 data (GSM) and the final solution comprises the full Ocean and Atmosphere signal. After restoring the GAD product, the result does not represent the ocean mass only.

Therefore, other products of the ocean surface pressure component (denoted as GAA) are subtracted from GAD product and then the ocean mass times series are estimated (Uebbing, B. et al., 2019).

3.1.1 Degree 2 order 0 coefficients (Earth oblateness)

The spherical harmonic coefficients of degree 2 and order 0 (C_{20}) is the representation of the flattening of the Earth. The C_{20} coefficients derived from GRACE data does not properly represent the flattening as the GRACE satellite has a polar orbit with inclination of 89^0. Thus, it cannot capture the Earth oblateness correctly (Cheng and Ries, 2017). Cheng and Ries, 2017 describe this variation as shown in Figure 3.1, from the figure approximately 160-day period, there is a large variation of GRACE estimation for C_{20}. Therefore, the C_{20} from the Satellite Laser Ranging data is used instead.

In this study, the monthly estimates of Satellite Laser Ranging of C_{20} produced by the Centre for Space and Research (CSR) were used to replace the C_{20} of GRACE data. This Satellite Laser Ranging C_{20} coefficients are found from analysis of Satellite Laser Ranging tracking data of five geodetic satellites including Ajisai, Stella, LAser GEOdynamics Satellite-1(LAGEOS-1), LAGEOS-2 and Starlette (Cheng and Ries, 2017).

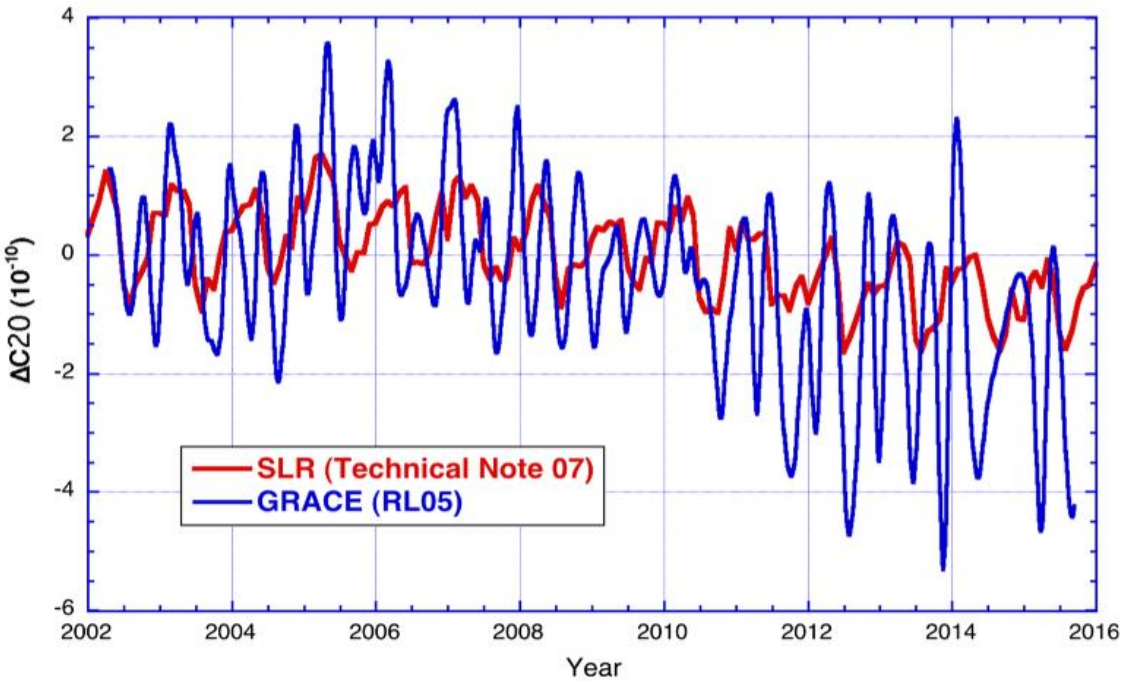

Figure 3.1: The variations in C_{20} from Satellite Laser Ranging and GRACE CSR-Release 05 (Source: Cheng and Ries, 2017).

3.1.2 Degree 1 coefficients (Geocenter Motion)

The GRACE satellite with its relative measurement concept does not sense spherical harmonic coefficients of degree 1. The GRACE level-2 data lack the three degree 1 (C_{10} , C_{11} and S_{11}) coefficients which are desired for complete representation of the mass redistribution of the Earth system. The degree 1 coefficients are defined as the motion of centre of mass of the Earth system with respect to the centre of the figure of solid surface (Sun et al. 2016).

Swenson et al. (2008) develops a method to estimate the degree 1 based on GRACE data and ocean and atmospheric models (Ocean Bottom Pressure). Then Sun et al., (2016) extended the method to include the effects of barystatic sea level fingerprint (that is solving the sea level equation using land mass changes as measured by GRACE) in ocean mass contribution to degree 1. Figure 3.2 shows the results of time series of degree 1 based on Sun et al., (2016) method after restoring atmosphere and ocean signal using GAC products. More details on this method can be found at (Sun et al. 2016).

In this study the degree 1 gravity coefficients were added back to GRACE data to correct for the geocenter motion and the file data contains the estimates of degree 1 gravity coefficients for GRACE Release 06 data (Swenson et al. 2008; Sun et al. 2016).

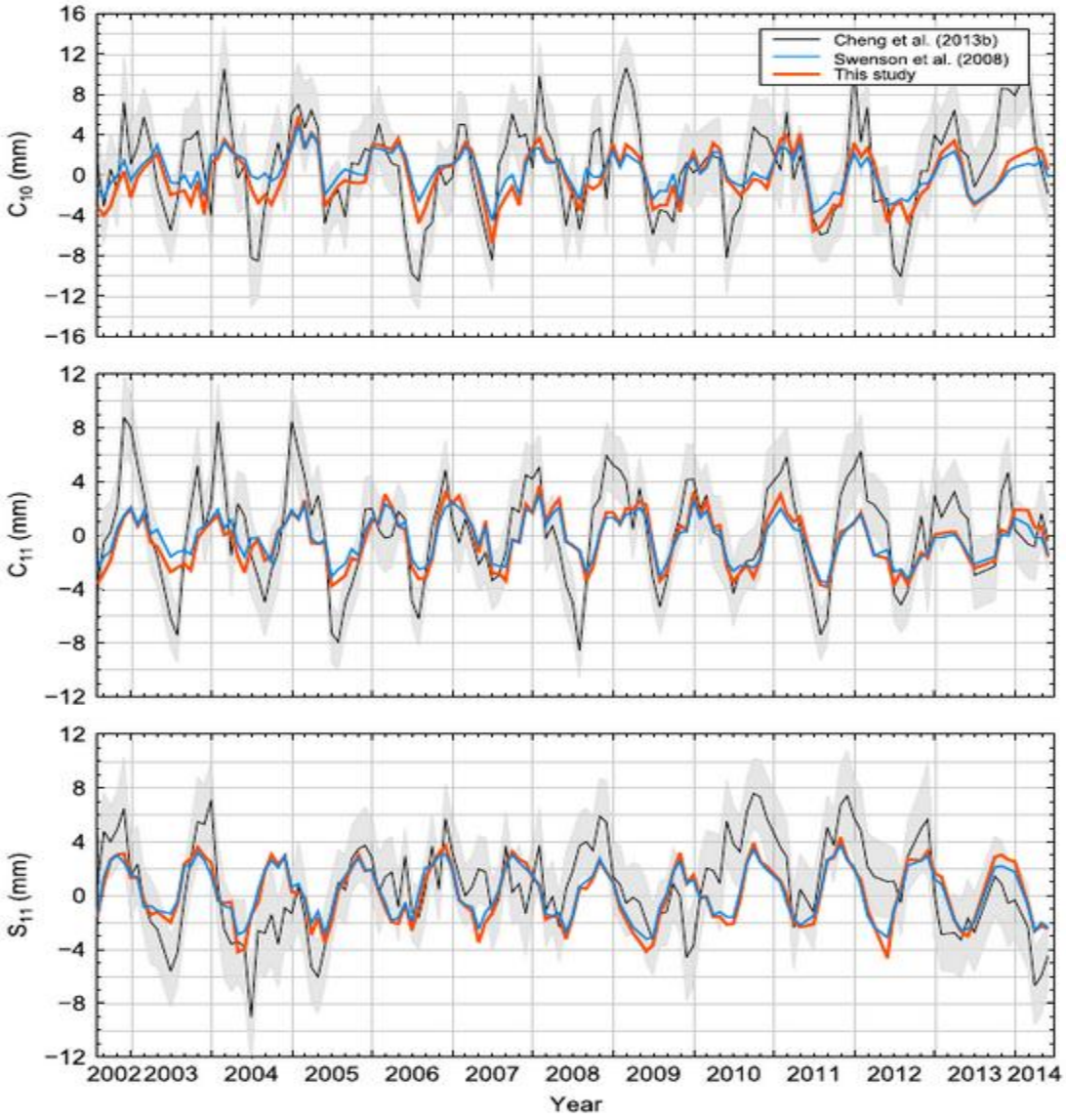

Figure 3.2: The degree 1-time series based on sun et al (2016) shown in red colour, previous based on Swenson et al (2008) and Satellite Laser Ranging solution by Cheng et al., (2013b). In the legend, "this study" refers to the study by Sun et al (2016) (source: Sun et al (2016).

3.1.3 Data filtering

When processing the GRACE data there is presence of North south stripes. The presence of these stripes indicated a high degree of spatial correlation in errors (Swenson and Wahr., 2006). Swenson and Wahr (2016) designs a filter to remove the correlation in spherical harmonic coefficients and apply the filter to the GRACE data.

Meanwhile, the higher spatial resolution in GRACE data is achieved with the increasing degree *l* and order *m* at the same time the gravity potential signal decreases continuously and short wavelength weaken more than longer wavelength. The Gaussian filter function radius of 350km

was used in this study to filter out the higher degree to improve the signal to noise ratio (Wahr et al 1998).

3.2 Satellite Altimetry data

The Sea Level Anomaly (SLA) data from satellite altimetry was used for further analysis of the trend in the Arctic region. The SLA is obtained by taking the difference between actual Sea Surface Height (SSH) and the Mean Sea Surface Height (MSSH). The SLA data is provided by Technical University of Denmark (DTU) in monthly grids from September 1991 to September 2018. These data are available at (https://ftp.space.dtu.dk/pub/ARCTIC_SEALEVEL/DTU_TUM_V3_2019/).

These data are based on the four European Space Agency (ESA) radar altimetry missions such as European Remote Sensing Satellite-1 (ERS-1), ERS-2, Environmental Satellite (Envisat) and Cryosat-2. The data are already corrected for all geophysical corrections (Rose, S.K. et al. 2019). For the comparability with GRACE data, only SLA data with the same period of GRACE were used in this study.

3.3 Precipitation data

The precipitation plays a role in the Arctic Ocean and all seas around, carefully studying the precipitation trend over the ocean, we will have a complete analysis of rainfall available over the entire Arctic region. The Global Precipitation Climatology Project (GPCP) data includes the observations from Satellites and gauge stations to estimate the monthly rainfall on the global grid of 2.5^0 by 2.5^0 latitude and longitude from 1979 to present (Adler et al. 2003).

The GPCP version 2.3 data set was used in this study, the data with the same period of GRACE was used for analysis. These data set is available at (https://www.ncei.noaa.gov/data/global-precipitation-climatology-project-gpcp-monthly/access/).

3.4 Boundaries of Arctic Ocean and all Seas

The exact boundary (shapefile) of the Arctic Ocean and all Seas used in this thesis was downloaded from International Hydrographic Organisation (IHO) Sea areas. The data set was composed by the Flanders Marine Data and Information centre (https://www.marineregions.org/downloads.php). The data represents the boundaries of the major oceans and sea of the world. The source for the boundaries is the publication 'Limits of Oceans and Seas' Special Publication No. 23 published by IHO in 1953 (Flanders Marine Institute, 2018).

The current IHO sea areas version 3 data set was used in this study and this shapefile helps to get the Latitude and Longitude of the Arctic Ocean and all Seas within the Arctic region. The Figure 3.3 below shows the boundary of major oceans and seas.

Source: (https://www.marineregions.org/images/boundaries/IHO_crop_small.png)

Figure 3.3: The IHO Sea areas

Chapter 4

Data Processing

This chapter describes the estimation of ocean mass trend in the Arctic region from GRACE data. For this purpose, the monthly GRACE level-2 data from April 2002 to April 2017 (almost 15 years) for CSR centre and from April 2002 to April 2019 (almost 17 years) for GFZ centre are used. Similarly, the trend maps of Seal Level Anomaly and Precipitation are produced for the same period as GRACE for further analysis.

4.1 Equivalent Water Height derived from GRACE data

The time variable of Earth's gravity field can be expressed in terms of Equivalent Water Height (EWH), and the calculations is shown in equation 4.1 below (Wahr et al 1998).

$$EWH(\theta,\lambda)[t] = \frac{a_e \rho_{ave}}{3\rho_w} \sum_{l=0}^{L} \frac{2l+1}{1+k_l} \sum_{m=0}^{l} \bar{P}_{lm}(cos\theta) \times (\Delta C_{l,m}[t] cos\, m\lambda + \Delta S_{l,m}[t] sin\, m\lambda) \quad (4.1)$$

Where a_e is the semi-major axis of the Earth, θ and λ are the colatitude and the longitude, ρ_w is the density of water ($1000\ kgm^{-3}$), ρ_{ave} is the Earth's mean density ($5517\ kgm^{-3}$), k_l is the loading love number for the spherical harmonic function of degree l the first 200 terms are taken from (Wahr et al 1998), $\bar{P}_{lm}(cos\theta)$ is the normalized Legendre function of degree l and order m and $\Delta C_{l,m}[t]$, $\Delta S_{l,m}[t]$ are the time varying spherical harmonic coefficients of the gravitational potential of the Earth obtained after deducting a long term mean as shown in equation 4.2 below.

$$\Delta C_{l,m}[t] = \bar{C}_{l,m}[t] - \bar{C}_{lm}^{mean}\ and\ \Delta S_{l,m}[t] = \bar{S}_{l,m}[t] - \bar{S}_{lm}^{mean} \quad (4.2)$$

Where $\bar{C}_{l,m}$ and $\bar{S}_{l,m}$ are the fully normalized spherical harmonic coefficients from GRACE data. In this study the maximum degree of spherical harmonic used was up to 96^0.

The errors in GRACE results likely to grow into large as the number of degrees l increases, the sum obtained in equation 4.1 may lead to inaccurate results. Meanwhile, the higher spatial resolution is achieved with the increasing degree l and the gravity potential signal decreases continuous. The Gaussian filter function is used to filter out the higher degree to improve the signal to noise ratio. The equation 4.1 can be written as

$$EWH(\theta,\lambda)[t] = \frac{a_e \rho_{ave}}{3\rho_w} \sum_{l=0}^{L} \frac{2l+1}{1+k_l} \sum_{m=0}^{l} \bar{P}_{lm}(cos\theta) \times W_l(\Delta C_{l,m}[t] cos\, m\lambda + \Delta S_{l,m}[t] sin\, m\lambda) \quad (4.3)$$

Where W_l is the Gaussian filter function with smoothing radius of 350km (Wahr et al 1998).

4.2 Ocean mass trend

During GRACE level-1 processing, the effects of ocean and atmosphere redistributions are removed prior to accumulating and solving monthly normal equations. Since the ocean mass trend is estimated using the GRACE level-2 data, the so-called Atmosphere and Ocean 1B De aliasing (AOD1B) background models must be restored back before further analysis. The AOD1B provide a prior information about temporal variations of the gravity field of the Earth caused by global mass variability in the ocean and atmosphere. The forecast data is based on the analysis of operational high resolution global numerical weather forecast prediction (NWP) model from European Centre for Medium-Range Weather forecasts (ECMWF) and ocean bottom pressure from unconstrained simulation with Global ocean circulation model (MPIOM) (Dobslaw, H., et al. 2017; Uebbing, B. et al., 2019).

The individual processing centres reduce the modelled atmosphere and ocean mass distribution with the temporal resolution sampling of 3 hours. In this study the AOD1B Release 06 was used. Since we are dealing with ocean application the so-called "GAD" product was used to add the ocean bottom pressure (OBP) of the background models as shown in equation 4.4 below. The GAD product was added to original GRACE data and then the final solution comprises the full Ocean and Atmosphere signal. (Uebbing, B. et al., 2019).

$$OBP = GSM + GAD \tag{4.4}$$

Where *GSM* is the original GRACE level-2 data and *OBP* is the Ocean Bottom Pressure. Uebbing, B. et al., (2019) suggests that, to make the GRACE data consistent with altimetry and the applied modified inverse Barometric (MIB) correction, it is necessary to remove the surface pressure component called $\overline{GAA}$ (this is not available within the datasets) after restoring the GAD product. It was then suggested to modify the GAD products by subtracting its mean over the ocean (here denoted as $[GAD]_{ocean}$).

To compute the GAD mean over the ocean ($[GAD]_{ocean}$), the global grid of area size 0.5^0 by 0.5^0 latitude and longitude was defined, and the area fall inside the ocean was assigned to 1 and for the area over the land was masked to 0. Then these grids were transformed into the Spherical harmonic coefficients of the ocean. Finally, the mean of the ocean was computed using equation 4.5 below.

$$[GAD]_{ocean} = \frac{1}{\bar{O}_{00}} \sum_{l=0}^{L} \sum_{m=0}^{l} \bar{O}_{lm} GAD_{lm} \tag{4.5}$$

Where $\bar{O}_{lm}$ is the spherical harmonic coefficients over the ocean of degree *l* and order *m*, GAD_{lm} is the GAD product (full normalized spherical harmonic coefficients up to degree *l* and order *m* of 96^0) and $\bar{O}_{00}$ is the mass of the ocean. The results of the $[GAD]_{ocean}$ corrected to GRACE data give the ocean mass (*OcM*) signal similarly to modified inverse Barometric (MIB) corrected altimetry as shown in equation 4.6 below (Uebbing, B. et al., 2019).

$$OcM = GSM + GAD - [GAD]_{ocean} \tag{4.6}$$

Here *GSM* is the original GRACE level-2 data and *OcM* is the spherical harmonic coefficients with full ocean mass signal as processed above. All computations of ocean mass were done according to procedures described in section 4.1 above. Here instead of EWH, now *OcM* is used. The monthly degree 2 order 0 (C_{20}) coefficients of GRACE data were replaced with the degree 2 order 0 of Satellite Laser Ranging data (Cheng and Ries, 2017). Also, the degree 1 gravity coefficients were added back to GRACE data to correct for the geocenter motion (Swenson et al.2008; Sun et al. 2016).

4.2.1 Data filtering

When processing the GRACE data, there is presence of North south stripes. In this study, a filter developed by Swenson and Wahr (2006) was used to remove the correlated in spherical harmonic coefficients and applied to filter the GRACE data.

Meanwhile, the higher spatial resolution in GRACE data is achieved with the increasing degree l and order m at the same time. The gravity potential signal decreases continuous and short wavelength weaken more than longer wavelength. The Gaussian filter function radius of 350km was used in this study to filter out the higher degree to improve the signal to noise ratio (Wahr et al 1998).

4.2.2 The GIA correction

The Glacial Isostatic Adjustment (GIA) is the reaction of the solid Earth to the ice age losing mass that was there during ice age. This mass is gone, and the Earth is reacting, and the surface goes up. The GRACE satellite senses the changes of masses, but here is not due to mass changes and the fact is that it is due to post glacial rebound. So in this aspect, it must be modelled and removed from GRACE measurements data. There are different GIA models to remove the post glacial rebound. In this study, the GIA model correction was based on ICE-6G_D (VM5a) (Peltier, et al., 2018).

4.3 Ocean mass trends in the Arctic region

The boundary information of the basins used in this study is based on the data which represents the boundaries of the major oceans and sea of the world. The data set was composed by the Flanders Marine Data and Information centre (https://www.marineregions.org/downloads.php). The source for the boundaries is the publication ‘Limits of Oceans and Seas’ Special Publication No. 23 published by IHO in 1953 (Flanders Marine Institute, 2018). The current IHO sea areas version 3 data set was used in this study to get the locations of the Arctic Ocean and all Seas within the Arctic region. The table 4.1 below shows the basic division information of each basin.

Table 4.1: The basin division basic information

S/N	Basins	Coordinates (Latitude, Longitude)	Area (km^2)
1	Laptev Sea	75.4937^0N, 122.0066^0E	513,667
2	Kara Sea	75.4299^0N, 77.3924^0E	896,938
3	Barents Sea	74.7239^0N, 42.1178^0E	1,408,430
4	Greenland Sea	74.7239^0N, 8.3032^0W	1,186,456
5	Baffin Bay	74.5061^0N, 67.1217^0W	529,960
6	Hudson Bay	59.0359^0N, 84.8891^0W	832,649
7	Beaufort Sea	72.1392^0N, 136.8292^0W	431,132
8	Chukchi Sea	72.1392^0N, 156.9730^0W	346,259
9	East Siberian Sea	69.4799^0N, 159.3441^0E	633,067
10	Arctic Ocean	84.8649^0N, 5.2026^0W	5,120,993

The ocean mass time series in 10 basins shown in table 4.1 above was computed for each month and the annual linear trends of ocean mass variations was estimated. The seasonal mass variation of each basin was plotted from April 2002 to April 2017 (almost 15 years) for CSR centre and from April 2002 to April 2019 (almost 17 years) for GFZ centre. Their results are presented in chapter five and analysis of the results is discussed in chapter six.

4.4 Sea Level Anomaly

The SLA data used in this study is provided by Technical University of Denmark (DTU) in monthly grids from September 1991 to September 2018. They have calculated the SLA products over the entire Arctic region and most of actual geophysical corrections have been corrected including tides and atmospheric delays. These data are available at (https://ftp.space.dtu.dk/pub/ARCTIC_SEALEVEL/DTU_TUM_V3_2019/). The SLA data range between the 65^0N to 81.5^0N latitude and -180^0 to 180^0 longitude (Rose, S.K. et al. 2019).

The trend map of SLA for the same period of GRACE data (2002.04 to 2017.04) was computed and the trend patterns over the entire Arctic regions were investigated. The results of the SLA time series and trend map computed are presented in chapter five and analysis of the SLA is discussed in chapter six.

4.5 Precipitation

For the mass variations in the ocean and over the land, precipitation also play important role in positive and negative trends of the Arctic region basins. This leads to computing and analysing the trends of precipitation over the study period of GRACE data (i.e., 2002 - 2017). The Global Precipitation Climatology Project (GPCP) data was downloaded from (https://www.ncei.noaa.gov/data/global-precipitation-climatology-project-gpcp_monthly/access/) the data include the observations from Satellites and gauge stations to estimate the monthly rainfall on the global grid of 2.5^0 by 2.5^0 latitude and longitude from 1979 to present (Adler et al,. 2003).

Chapter 5

Results

This chapter presents the results obtained after processing the GRACE level-2 data from both GFZ and CSR centres. The time series of all ten basins are displayed and the detailed long-term trend for the entire study period is presented from both centres. The means of the solutions from CSR and GFZ centres were taken as a final solution. Finally, the results from processing the Sea Level Anomaly and the Precipitation are also presented.

5.1 Results of the Ocean mass trend Map from GFZ and CSR centre

The long-term linear trend of the ocean mass for the period 2002.04 to 2019 (GFZ) and 2002.04 to 2019 (CSR) are shown in the Figure 5.2 and 5.3 respectively with the resolution of 0.5^0 by 0.5^0, the positive trend is presented with blue colour and the negative trend with red colour while zero trend with white colour. The map of Arctic region with basins (Seas) division is shown in Figure 5.1, the boundary is based on the data which represents the boundaries of the major oceans and sea of the world as discussed in chapter 04 section 4.3.

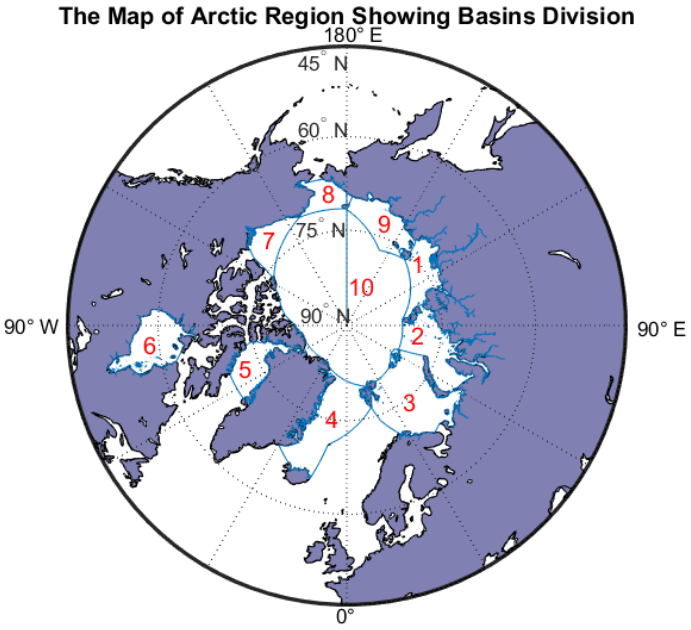

Figure 5.1: The map of arctic region showing the basins division, numbers refer (1) Laptev Sea, (2) Kara Sea, (3) Barents Sea, (4) Greenland Sea, (5) Baffin Bay, (6) Hudson Bay, (7) Beaufort Sea, (8) Chukchi Sea, (9) East Siberian, (10) Arctic Ocean.

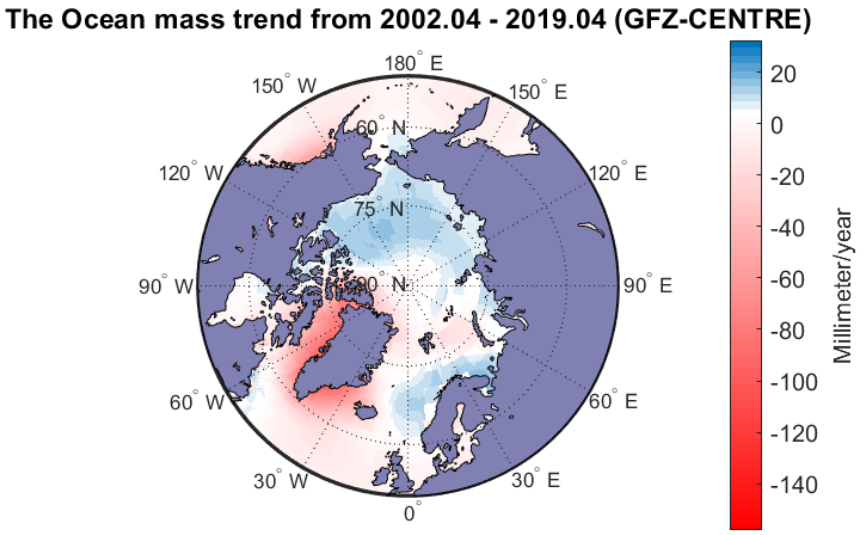

Figure 5.2: The Ocean mass trends map from GFZ centre.

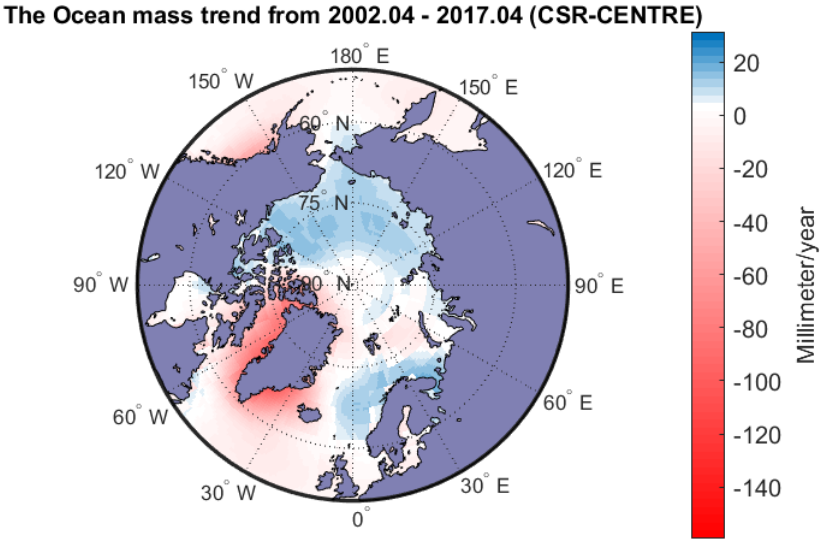

Figure 5.3: The Ocean mass trends map from CSR centre.

5.2 Results of the ocean mass time series from GFZ centre

The ocean mass time series and annual linear trends of all 10 basins are estimated from the GFZ centre and plotted from April 2002 to April 2019 as shown in Figure 5.4 to 5.6, respectively. The time series of Laptev Sea has a positive trend with ocean mass gain of 6.66 mm/year for the periods of April 2002 to April 2019. Kara Sea has a positive trend with ocean mass gain of 4.08 mm/year for the periods of April 2002 to April 2019. Hudson Bay has a positive trend with ocean mass gain of 0.25 mm/year for the periods of April 2002 to April 2019. Beaufort Sea has a positive trend with ocean mass gain of 7.73 mm/year. East Siberian Sea has a positive trend with ocean mass gain of 7.89 mm/year for the periods of April 2002 to April 2019. Arctic Ocean has a positive trend with ocean mass gain of 5.95 mm/year for the periods of April 2002 to April 2019.

The time series of Barents Sea has a negative trend with ocean mass loss −0.63 mm/year for the periods of April 2002 to April 2019. The time series of Greenland Sea has a negative trend with ocean mass loss −8.44 mm/year for the periods of April 2002 to April 2019. The time series of Baffin Bay has a highest negative trend with ocean mass loss −58.08 mm/year for the periods of April 2002 to April 2019.

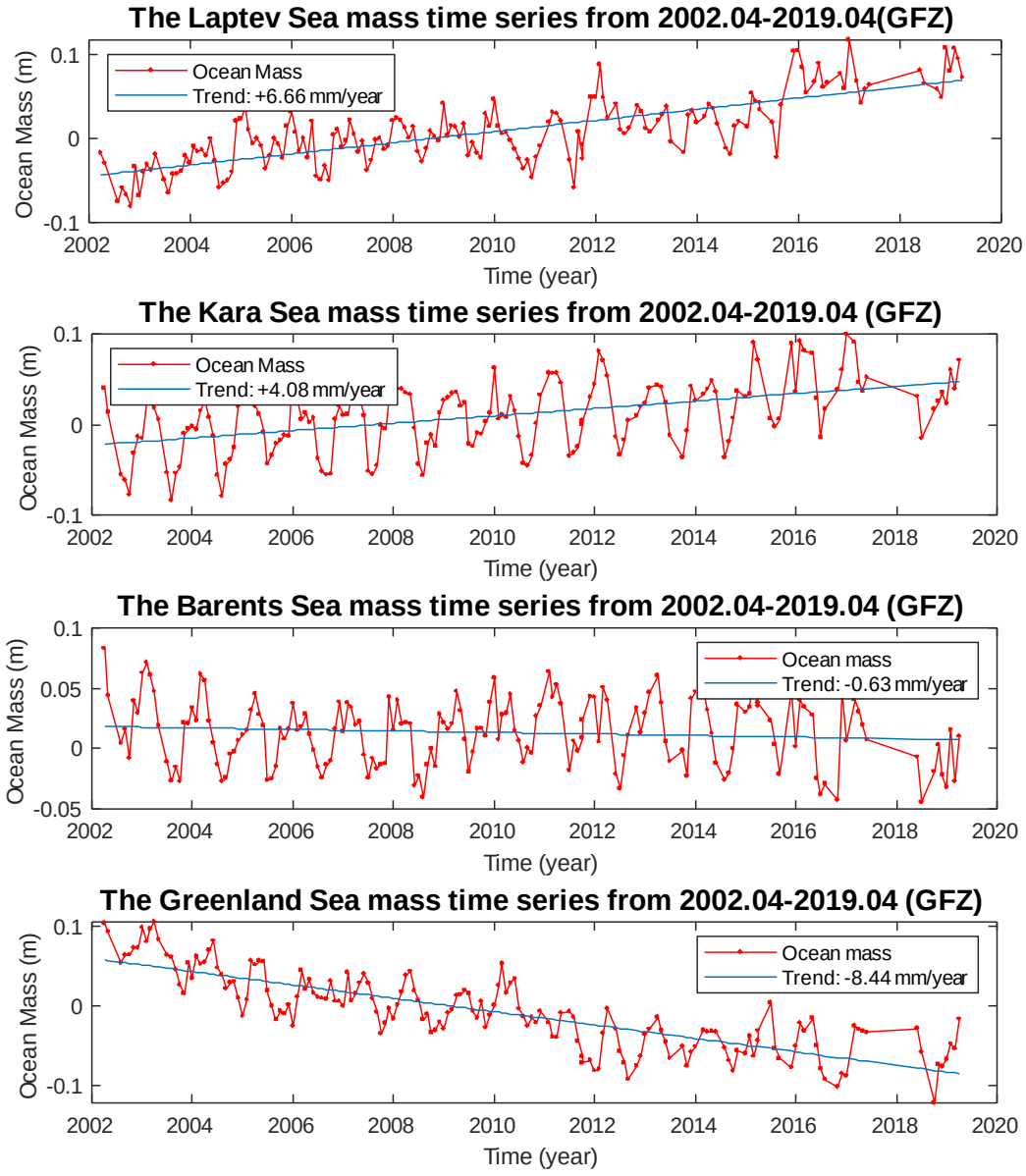

Figure 5.4: The Ocean mass time series of Laptev sea, Kara Sea, Barents Sea and Greenland Sea respectively from April 2002 to April 2019 from GFZ centre

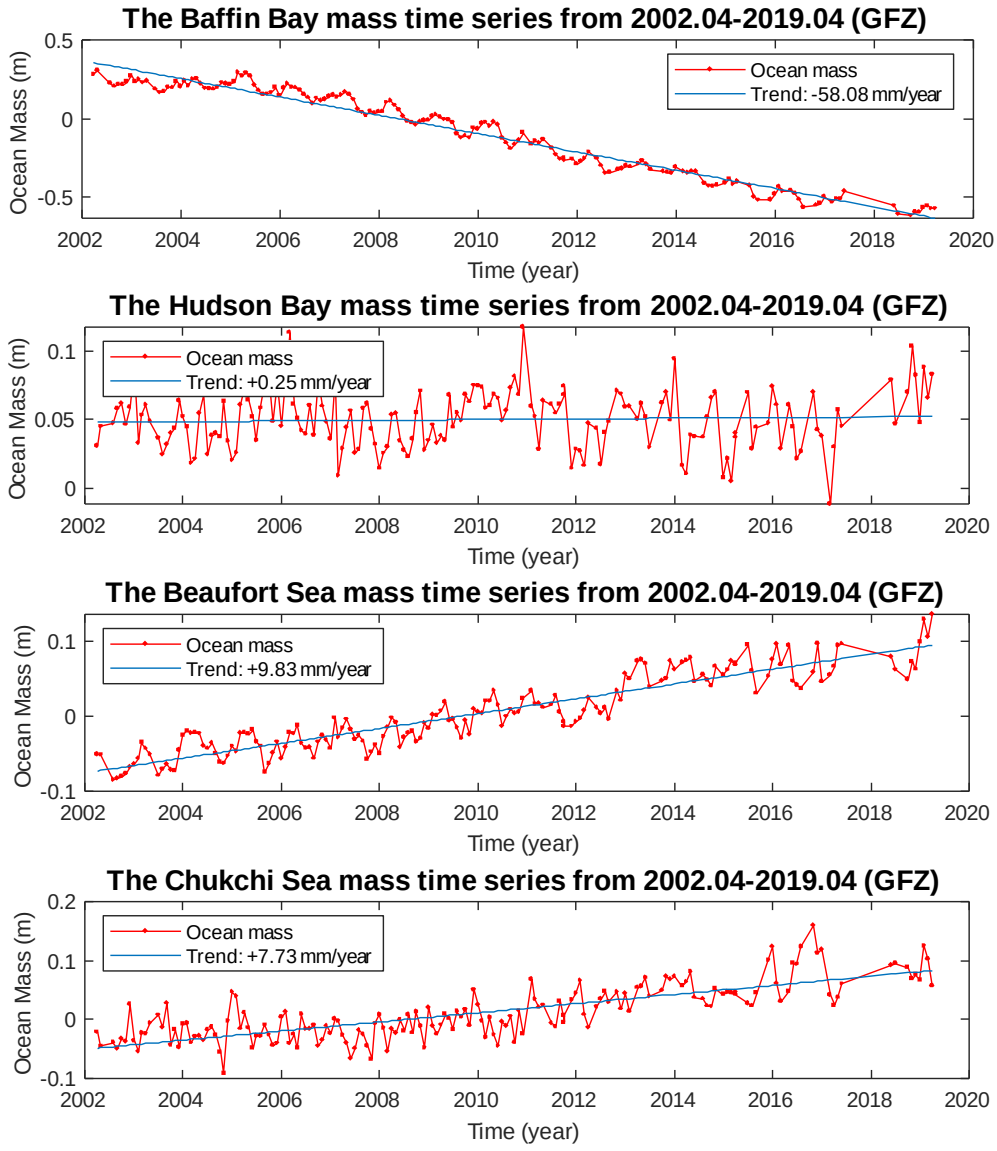

Figure 5.5: The Ocean mass time series of Baffin Bay, Hudson Bay, Beaufort Sea and Chukchi Sea respectively from April 2002 to April 2019 from GFZ centre

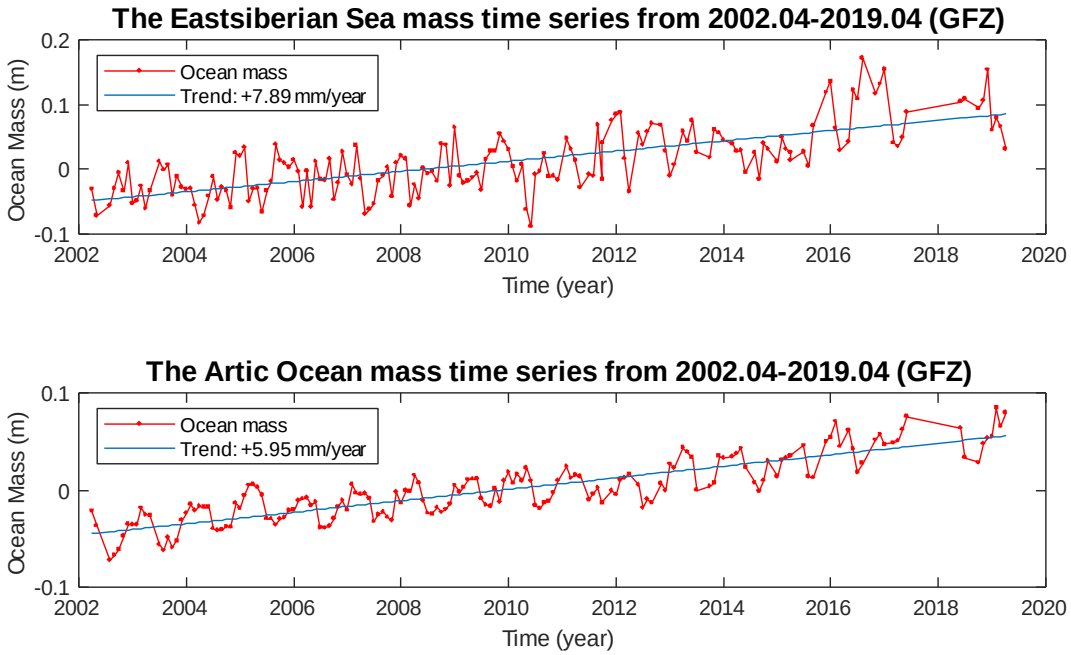

Figure 5.6: The Ocean mass time series of East Siberian and Arctic Ocean respectively from April 2002 to April 2019 from GFZ centre

5.3 Results of the Ocean mass time series from CSR centre

The ocean mass time series and annual linear trends of all 10 basins were estimated from the CSR centre as shown in Figure 5.7 to 5.9 respectively below. The time series of Laptev Sea has a positive trend with ocean mass gain of 7.41 mm/year for the periods of April 2002 to April 2017. Kara Sea has a positive trend with ocean mass gain of 2.99 mm/year for the periods of April 2002 to April 2017. The times series of Barents Sea has a positive trend with ocean mass gain of 0.28 mm/year for the periods of April 2002 to April 2017. Hudson Bay has a positive trend with ocean mass gain of 1.10 mm/year for the periods of April 2002 to April 2017. Beaufort Sea has a positive trend with ocean mass gain of 10.19 mm/year. East Siberian Sea has a positive trend with ocean mass gain of 8.81 mm/year for the periods of April 2002 to April 2017. Arctic Ocean has a positive trend with ocean mass gain of 5.97 mm/year for the periods of April 2002 to April 2017.

The time series of Greenland Sea has a negative trend with ocean mass loss -8.89 mm/year for the periods of April 2002 to April 2017. The time series of Baffin Bay has a highest negative trend with ocean mass loss -59.90 mm/year for the periods of April 2002 to April 2017.

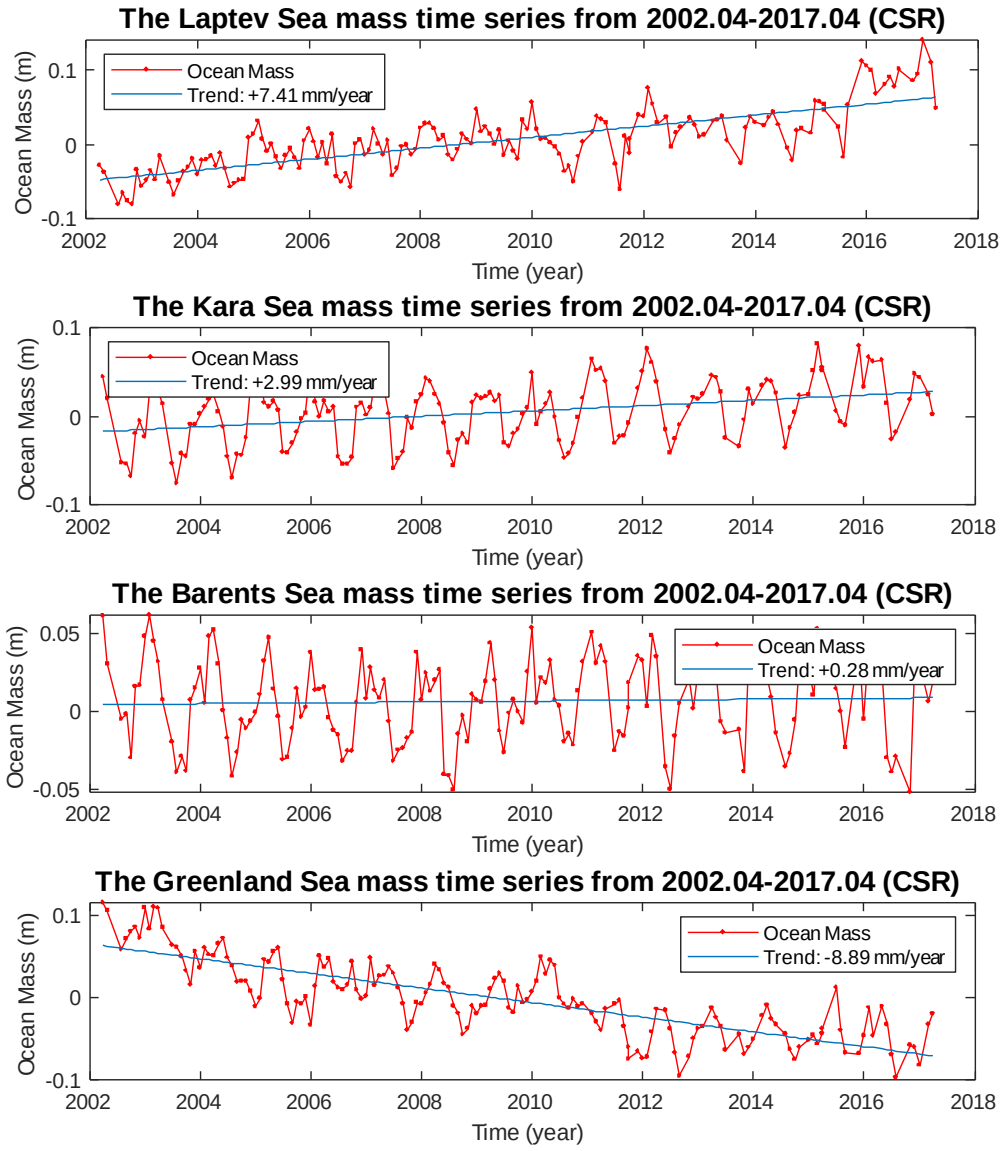

Figure 5.7: The Ocean mass time series of Laptev sea, Kara Sea, Barents Sea and Greenland Sea respectively from April 2002 to April 2017 from CSR centre

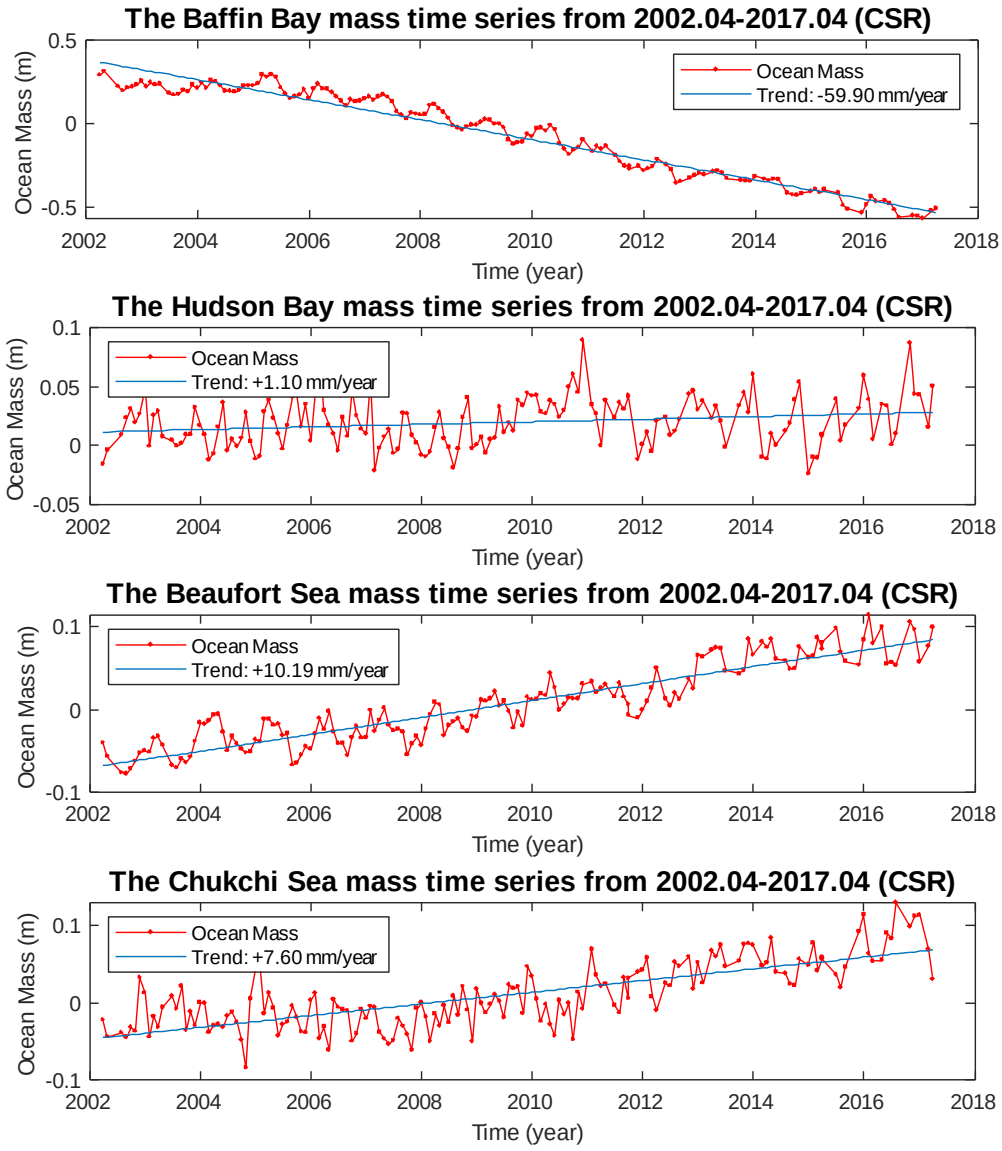

Figure 5.8: The Ocean mass time series of Baffin Bay, Hudson Bay, Beaufort Sea and Chukchi Sea respectively from April 2002 to April 2017 from CSR centre

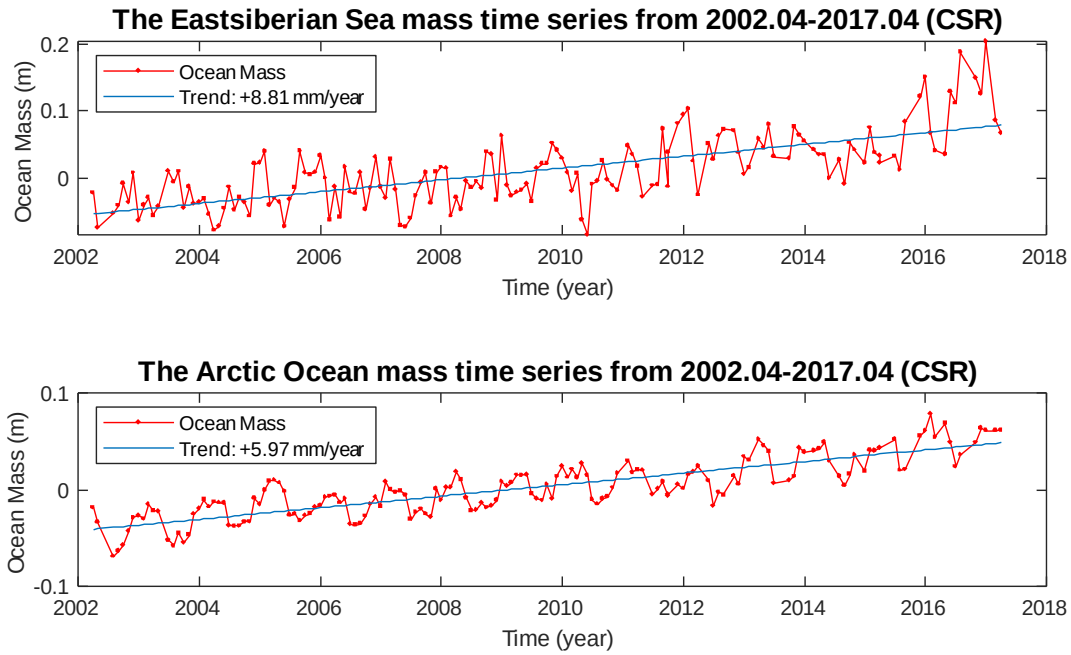

Figure 5.9: The Ocean mass time series of East Siberian and Arctic Ocean respectively from April 2002 to April 2017 from CSR centre

5.4 Results from the mean of solutions from GFZ and CSR centres

The monthly global grid from GFZ and CSR centre was then combined by calculating the mean value of each month and recomputed the monthly time series of each basins and the results of the time series are attached at Appendix I. Also, the annual trends were computed by mean of least square adjustment. The results of trends estimated are summarized in table 5.1 below. The long-term linear trend of the ocean mass for the period 2002.04 to 2017 is shown in the Figure 5.10 with the spatial resolution of 0.5^0 by 0.5^0. The positive trend is presented with blue colour and the negative trend with red colour while zero trend with white colour. The analysis of these trends is discussed in detail in chapter 06.

Table 5.1 The mean of monthly ocean mass from GFZ and CSR centres

S/N	**Basins**	**Ocean mass trend (mm/year) 2002.04 - 2017.04**
1	Laptev Sea	+6.83
2	Kara Sea	+3.73
3	Barents Sea	+0.13
4	Greenland Sea	−9.10
5	Baffin Bay	−59.58
6	Hudson Bay	+0.35
7	Beaufort Sea	+9.99
8	Chukchi Sea	+7.64
9	East Siberian Sea	+8.25
10	Arctic Ocean	+5.83

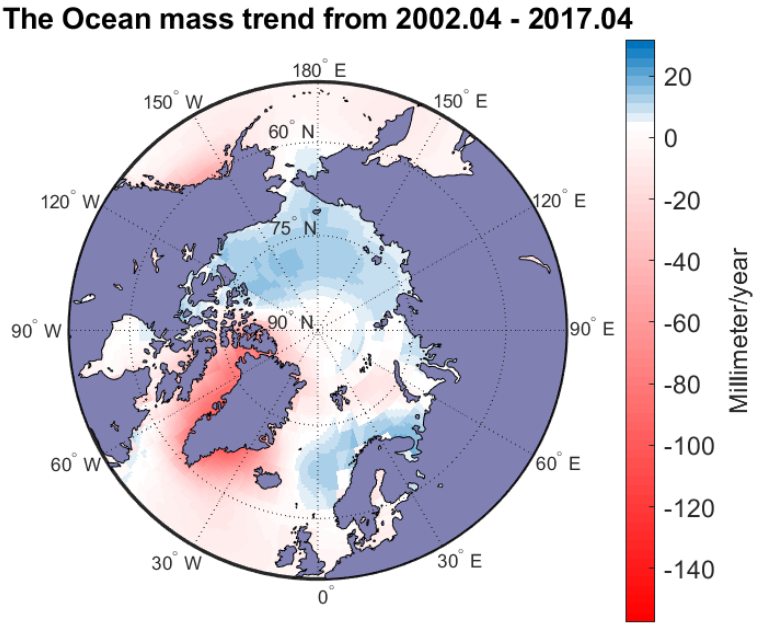

Figure 5.10: The Ocean mass trends map.

5.4 The results Arctic Sea Level Anomaly

The long-term trend of Sea Level Anomaly data over the entire Arctic region was calculated and the result is shown in the Figure 5.11 below. The inclination of the satellite Altimetry ranges between 81^0 and 82^0 would dictate a spatial coverage up to 82^0 and that is what exactly seen in the Figure 5.11. We have only data cover from latitude $65^0\ N$ to $81.5^0\ N$ and the whole range of longitude ($180^0\ W$ to $180^0\ E$) and the data cover the same period of GRACE data from April 2002 to April 2017 so that the things get more comparable. The positive trend is presented with

blue colour and the negative trend with red colour while zero trend with white colour. The analysis of these trends is discussed in detail in chapter 06.

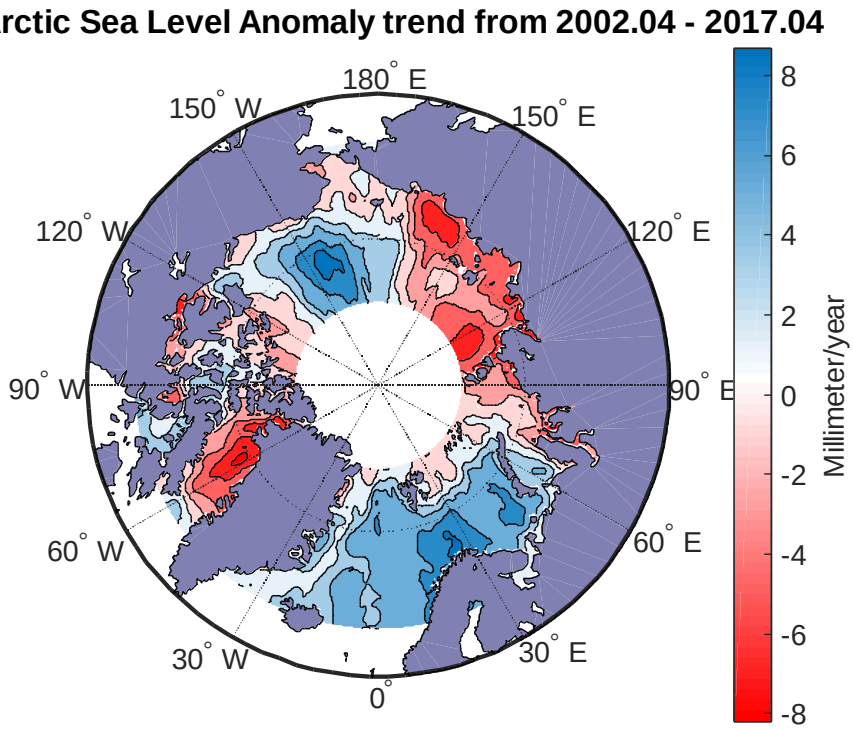

Figure 5.11: The Arctic Sea Level Anomaly trend map

The mean value for each month of the Sea Level Anomaly data of the entire Arctic region was calculated and their monthly time series was plotted from April 2004 to April 2017 as shown in Figure 5.12 below. From the Figure 5.12, over the entire study period mostly a low Sea Level is seen from March to May in each year and a high Sea Level is seen from September to November in each year. The linear trend of the time series was computed by means of Least square adjustment and over the entire study period have a positive trend of +2.69 mm/year.

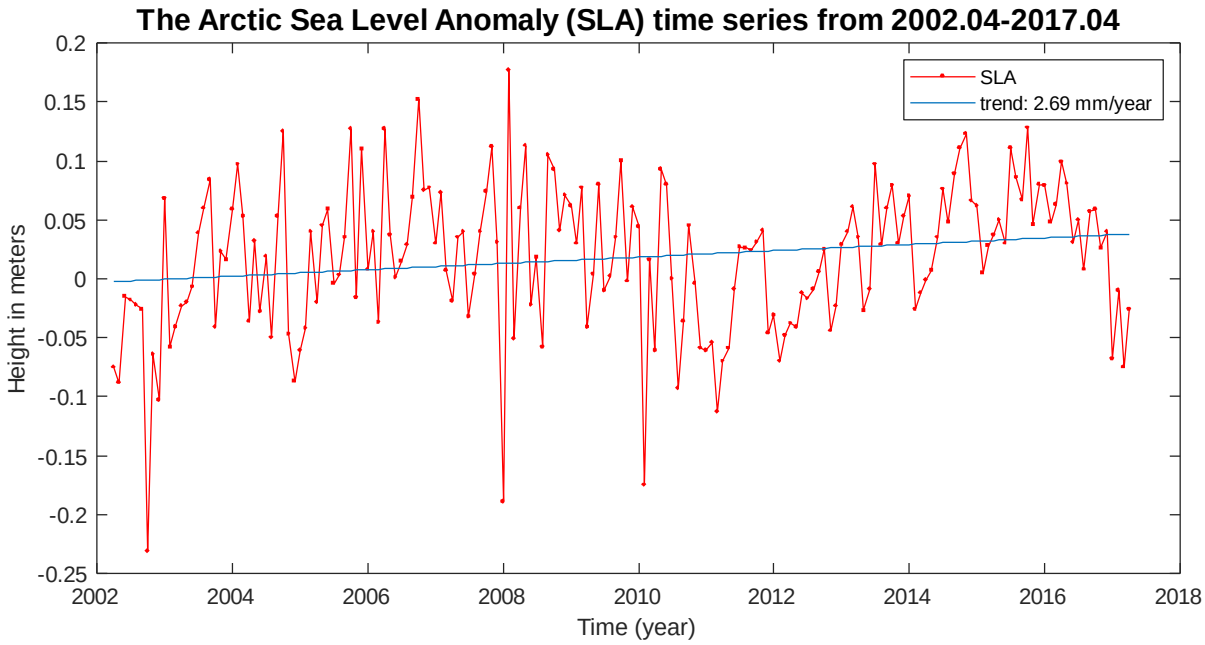

Figure 5.12: The Arctic sea level anomaly time series

5.5 The results of precipitation trend

The long-term linear trend of the Precipitation for the period 2002.04 to 2017 is shown in the Figure 5.13 with the spatial resolution of 2.5^0 by 2.5^0. The positive trends are presented with blue colour and the negative trend with red colour while zero trend with white colour. The analysis of these trends is discussed in detail in chapter 06.

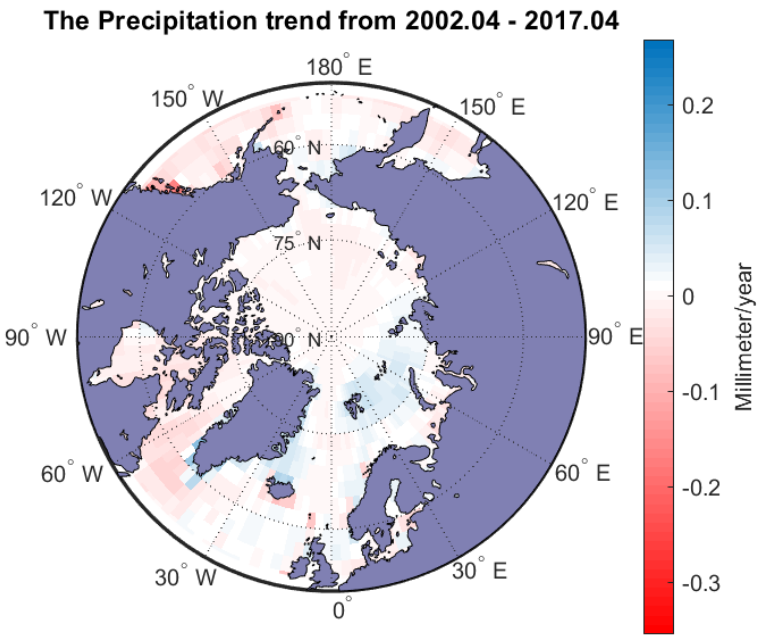

Figure 5.13: The Precipitation trend map from 2002.04 to 2017.04

Chapter 6

Analysis of the Results

6.1 Analysis of the ocean mass trends and SLA trends

The strong negative trends seen in Figure 6.1 around the Greenland are mainly caused by the issue of loss of gravitation attraction of the lost Greenland masses. The Greenland ice sheet (heavy mass) exerts the gravitational force that attracts the surrounding sea water (small mass). The Greenland losses ice mass because of atmospheric warming (Shepherd, A. et al., 2019). When the Greenland losses ice mass, the results in loss of gravitational attraction and the ocean water that was attracted also spread out as well. This effect affects regional sea level that is why, closed to Greenland, we have strong negative trends on Baffin Bay in west of Green land, south and south east of Greenland (Brunnabend S.-E., et al. 2011).

The Greenland Sea has negative trend in ocean mass of -9.10 mm/year and Sea Level Anomaly trend is negative at north of -1 mm/year and positive trend up to 6mm/year. The positive trend in Sea Level Anomaly close to the Greenland is questionable and can be attributed to the few data existence during ERS-1 or ERS-2 or Envisat period due to heavy sea ice coverage. Whereas the same area Cryosat-2 provides a narrow strip of SARin data (Anderson OB and Piccini G. 2016). The negative trend in mass of Greenland Sea is influenced by gravitational attraction of Greenland masses or due to freshwater outflow from the Arctic ocean through western side of Fram Strait to North Atlantic ocean (Timmernans and Marshahall., 2020 and Brunnabend S.-E., et al. 2011).

The Baffin Bay has the strongest negative trend in ocean mass of -59.59 mm/year and Sea Level Anomaly trend of approximately -9 mm/year. These negative trends could be due to the gravitational attraction of Greenland masses (Brunnabend S.-E., et al. 2011). Also, the freshwater from melting of ice from the land. In the Baffin Bay, the Arctic ocean freshwater outflow passes through it on the way to North Atlantic Ocean (Rose, S.K. et al. 2019).

The Beaufort Sea has the highest positive trends in ocean mass of 9.99 mm/year and Sea Level Anomaly of approximately to 10 mm/year. The positive trends are influenced by the presence of Beaufort Gyre, in which the Anticyclone winds and Ekman transport accumulate the fresh water and come up like an arc. This could be the reason for the positive trends in this region (Rose, S.K. et al. 2019). Another reason for the positive trend in this region is the pacific ocean water inflow into the arctic Ocean through Bering strait at approximately 50m deep and 80km wide. Below the surface mixed layer (less than 50m deep) is relatively warm near surfaces in the Canadian basin. This layer with Pacific ocean origin has a temperature range between -1 to $1\ ^{0}$C lies at depth roughly 50m to 100m in Canadian basin. It is called summer Pacific summer water since it ventilates during summer. Beneath the summer pacific water layer lies the pacific winter water

which ventilates to this region in winter and they are cooler and saltier water. Below the pacific water lies the Atlantic water origin with temperature range from 0 to 3 ^{0}C at depth approximately 150 to 500m (Timmernans and Marshahall., 2020; Woodgate, R. (2013)).

The Chukchi Sea has positive trend in ocean mass of 7.64 mm/year and Sea Level Anomaly trend range from −1 mm/year and 1 mm/year. The positive trends are most probably influenced by presence of Pacific Ocean summer water in the Chukchi shelf which are warmer and saltier. Moreover, the Pacific winter water which are colder and saltier resides in this area. The pacific winter water is produced by cooling and brine rejection when ice formation during winter. These processes result into increase in ocean mass (Timmernans and Marshahall., 2020; Yi, S., et al. (2019). The partially negative trend in Sea Level anomaly could be influenced by the sea ice melt or runoff usually in the upper part of water column (usually shallower than 15m) (Yi, S., et al (2019).

The Hudson Bay has positive trend in ocean mass of 0.35 mm/year and Sea Level Anomaly trend range from 1 to 3 mm/year. It is the area of high Glacial Isostatic Adjustment values, the positive trends are due to large input of fresh water from river and precipitation, ice melting influenced by air temperature and inflow of Arctic Ocean waters (Andrews, J. et al. 2018).

Barents Sea has from −1mm/year to 7mm/year. The positive trends here are influenced by the inflow of Atlantic water which are warm, saltier, and denser into the Arctic ocean (Timmernans and Marshahall., 2020).

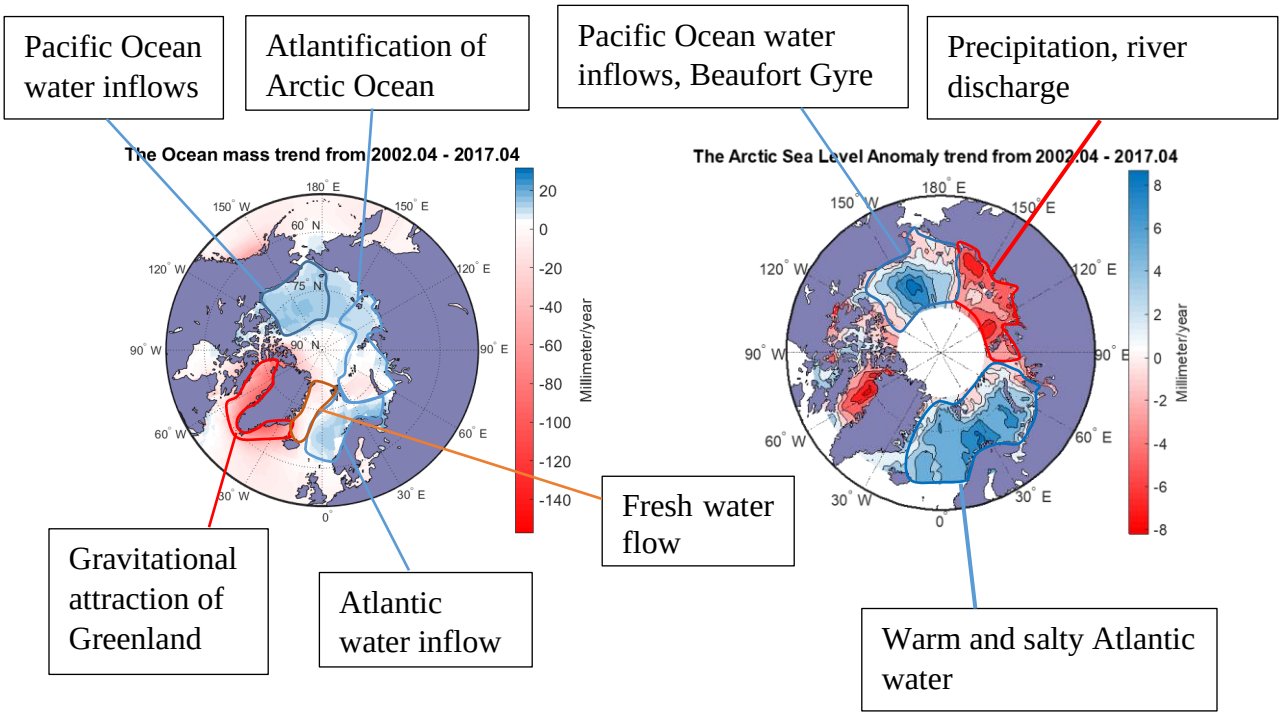

Figure 6.1: Annotated Ocean Mass trend (a) and Sea Level Anomaly trend (b)

Kara sea has positive trend in ocean mass of 3.73 mm/year, Laptev sea has positive trend in ocean mass of 6.83 mm/year, East Siberian Sea has a positive trend of 8.25 mm/year and Arctic ocean has positive ocean mass trend of 5.83 mm/year. The positive trends in this region are influenced by the inflow of Atlantic water into Arctic ocean and have created changes including weaker stratification, reduced sea ice and accelerates the Atlantic water layer heat fluxes further Northeast into Eurasian Basin and renamed as Atlantification of Arctic ocean (Polyakov et al., 2017). The Atlantic water is transferred into Arctic ocean through Fram Strait (or may be through Barents Sea) into deep ocean and these are warm and salty waters (salty than in arctic water). Because of this process, if the salt is in water it increases the mass of the ocean (Polyakov et al., 2017 and Polyakov et al., 2020). The Kara Sea, Laptev Sea and East Siberian sea all have negative trends range from -2 mm/year to -6 mm/year. These negative trends of Sea Level Anomaly in this region are influenced by the gain of fresh water, net precipitation, run off increased and more discharge from the land to the sea water (Rose, S.K. et al. 2019).

6.1.1 Analysis of Precipitation

This is very uncertain data sets; this precipitation data is not reliable because most of the data are satellite-based data and most of precipitation in the Arctic region is kind of solid precipitation or snow in fact. In that aspect the positive or negative trend seen in Figure 6.2 could not be much reliable, although we get a trail and get a result. From Figure 6.2 the positive trend in precipitation found in north of Barents Sea and Kara sea up to 0.1 mm/year, also in east of Greenland Sea the trend ranges from 0 to 0.1 mm/year. The remaining seas have negative trend in precipitation ranges from 0 to -0.1 mm/year.

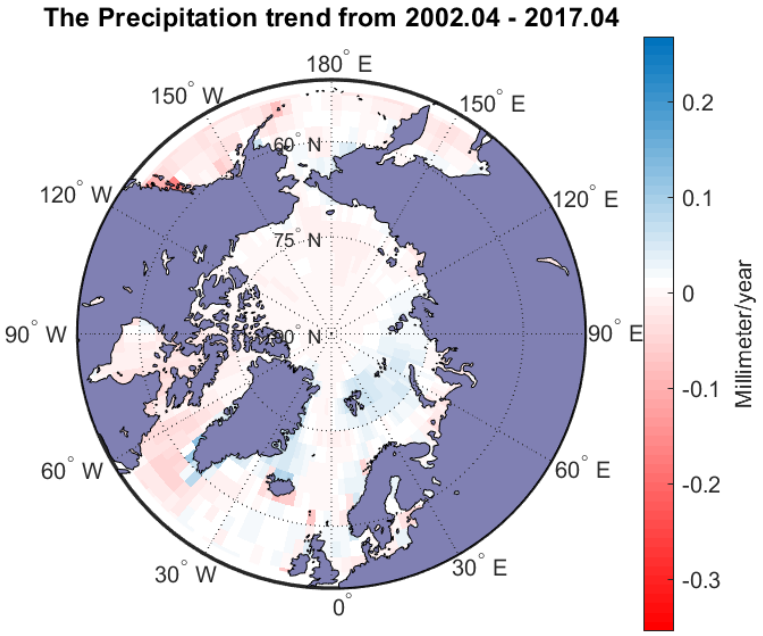

Figure 6.2: The Precipitation trend map from 2002.04 to 2017.04

6.2 Analysis the effects of Degree 2 and Degree 1

We replace the C_{20} with the degree 2 of Satellite Laser Ranging data because the GRACE satellite has a polar orbit with inclination of 89^0. It cannot capture the Earth oblateness properly (Cheng and Ries, 2017). It is known that the GRACE satellite is a relative orbit and the degree 1 is the representation of the centre of mass of the Earth in principle. Since the GRACE satellite is a relative orbit does not sense degree 1 (centre of mass) at all that is why we take degree 1 from external source and added back to GRACE data (Swenson et al.2008; Sun et al. 2016).

So far, we have performed all results from GRACE data with replacement of C_{20} to correct for Earth oblateness and the degree 1 coefficients were added back to GRACE data to correct for the geocenter motion. We want to investigate the trends of Ocean mass if the GRACE data are processed without replacing the C_{20} and analysing the results of trends basically comes from the fact that the C_{20} is changed. Also, another investigation was to find out what happens if we do not add back the degree 1 into GRACE data.

Here we have four cases, in case 01 the C_{20} replaced and degree 1 added the results are shown in table 6.1 and the trend map is shown at Appendix II from GFZ and CSR centres. In Case 02 the C_{20} is not replaced but the degree 1 is added, where the results are shown in table 6.2 and the trend map is shown at Appendix III from GFZ and CSR centres. In Case 03 the C_{20} is not replaced and degree 1 is not added and the results are shown in table 6.3 and the trend map is shown at Appendix IV from GFZ and CSR centres. In Case 04 the C_{20} replaced and degree 1 is not added, where the results are shown in table 6.4 and the trend map is shown at Appendix V from GFZ and CSR centres.

To evaluate the effect of the C_{20} and degree 1 on the GRACE data, the results of trend of Case 01 were taken as the reference. Then the differences in trend for each basin were computed and the results are shown in Tables 6.2, 6.3 and 6.4, respectively. For the Ocean mass trend where C_{20} not replaced with SLR data and Degree 1 added, the differences in trend range between 0.99 to 1.69 mm/year from GFZ centre and between 1.08 to 1.84 mm/year from CSR centre. For the Ocean mass trend where C_{20} not replaced with SLR data and Degree not added, the differences in trend range between 2.92 to 3.92 mm/year from GFZ centre and between 3.22 to 4.27 mm/year from CSR centre. For the Ocean mass trend where C_{20} replaced with SLR data and Degree 1 not added, the differences in trend range between 1.74 to 2.30 mm/year from GFZ centre and between 1.90 to 2.49 mm/year from CSR centre.

Table 6.1: The Ocean mass trend where **C_{20}** Replaced with SLR data and Degree 1 added

S/N	Basins	GFZ (mm/year) 2002.04 - 2019.04	CSR (mm/year) 2002.04 - 2017.04
1	Laptev Sea	+6.66	+7.41
2	Kara Sea	+4.08	+2.99
3	Barents Sea	-0.63	+0.28
4	Greenland Sea	-8.44	-8.89
5	Baffin Bay	-58.08	-59.90
6	Hudson Bay	+0.25	+1.10
7	Beaufort Sea	+9.83	+10.19
8	Chukchi Sea	+7.73	+7.60
9	East Siberian Sea	+7.89	+8.81
10	Arctic Ocean	+5.95	+5.97

Table 6.2: The Ocean mass trend where **C_{20} not** Replaced with SLR data and Degree 1 added

S/N	Basins	GFZ (mm/year) 2002.04 - 2019.04	Differences GFZ (mm/year)	CSR (mm/year) 2002.04 - 2017.04	Differences CSR (mm/year)
1	Laptev Sea	+8.03	1.37	+8.91	1.50
2	Kara Sea	+5.52	1.44	+4.57	1.58
3	Barents Sea	+0.87	1.50	+1.93	1.65
4	Greenland Sea	-6.97	1.47	-7.29	1.60
5	Baffin Bay	-56.64	1.44	-58.33	1.57
6	Hudson Bay	+1.24	0.99	+2.18	1.08
7	Beaufort Sea	+11.20	1.37	+11.68	1.49
8	Chukchi Sea	+9.03	1.30	+9.01	1.41
9	East Siberian Sea	+9.27	1.38	+10.32	1.51
10	Arctic Ocean	+7.64	1.69	+7.81	1.84

Table 6.3: The Ocean mass trend where **C_{20} not** Replaced with SLR data and Degree 1 **not** added

S/N	**Basins**	**GFZ (mm/year) 2002.04 - 2019.04**	**Differences GFZ (mm/year)**	**CSR (mm/year) 2002.04 - 2017.04**	**Differences CSR (mm/year)**
1	Laptev Sea	+9.86	3.20	+10.90	3.49
2	Kara Sea	+7.58	3.50	+6.79	3.80
3	Barents Sea	+3.14	3.77	+4.37	4.09
4	Greenland Sea	-4.67	3.77	-4.79	4.10
5	Baffin Bay	-54.48	3.60	-55.96	3.94
6	Hudson Bay	+3.17	2.92	+4.32	3.22
7	Beaufort Sea	+13.06	3.23	+13.73	3.54
8	Chukchi Sea	+10.76	3.03	+10.92	3.32
9	East Siberian Sea	+11.09	3.20	+12.30	3.49
10	Arctic Ocean	+9.87	3.92	+10.24	4.27

Table 6.4: The Ocean mass trend where **C_{20}** Replaced with SLR data and Degree 1 **not** added

S/N	**Basins**	**GFZ (mm/year) 2002.04 - 2019.04**	**Differences GFZ (mm/year)**	**CSR (mm/year) 2002.04 - 2017.04**	**Differences CSR (mm/year)**
1	Laptev Sea	+8.49	1.83	+9.40	1.99
2	Kara Sea	+6.14	2.06	+5.21	2.22
3	Barents Sea	+1.64	2.27	+2.73	2.45
4	Greenland Sea	-6.14	2.30	-6.40	2.49
5	Baffin Bay	-55.92	2.16	-57.54	2.36
6	Hudson Bay	+2.18	1.93	+3.24	2.14
7	Beaufort Sea	+11.69	1.86	+12.24	2.05
8	Chukchi Sea	+9.47	1.74	+9.50	1.90
9	East Siberian Sea	+9.70	1.81	+10.79	1.98
10	Arctic Ocean	+8.18	2.23	+8.39	2.42

Chapter 7

Conclusion

The main objective of this thesis was to analyse the long-term variations of ocean mass in the Arctic region using Satellite gravimetry. The standard GRACE level -2 data from April 2002 to April 2017 (15 years) from GFZ and CSR centres were used to estimate the linear trends of Arctic ocean and all seas around it, the means of solutions were taken as final results. The Sea Level Anomaly data used in this study is provided by Technical University of Denmark (DTU) in monthly grids from September 1991 to September 2018 (Rose, S.K. et al. 2019). For the comparability, the trend map of SLA for the same period of GRACE data (2002.04 to 2017.04) was computed in the entire Arctic region.

According to the results, the Beaufort Sea has the highest positive trends in ocean mass of 9.99 mm/year and Sea Level Anomaly of approximately to 10 mm/year. The positive trends are influenced by the presence of Beaufort Gyre which the anticyclone winds accumulate the fresh water and deeper in this region there are cold and salty water from Pacific Ocean (Rose, S.K. et al. 2019 and Timmernans and Marshahall., 2020). The Chukchi Sea has positive trend in ocean mass of 7.64 mm/year and Sea Level Anomaly trend range from -1 mm/year to 1 mm/year. The positive trend is influenced by Pacific Ocean water which are warmer and saltier (denser than Chukchi sea) these processes result into increase in ocean mass (Timmernans and Marshahall., 2020).

The Baffin Bay has the strongest negative trend in ocean mass of -59.59 mm/year and Sea Level anomaly trend of approximately -9 mm/year. These negative trends are caused by the Gravitation attraction of Greenland masses (Brunnabend S.-E., et al. 2011). Also the fresh water from melting of ice from the Greenland and in the Baffin Bay, the Arctic ocean freshwater outflows through it on the way to North Atlantic Ocean (Rose, S.K. et al. 2019). The Hudson Bay has positive trend in ocean mass of 0.35 mm/year and Sea Level Anomaly trend range from 1 to 3 mm/year. The positive trends are due to large input of fresh water from river and precipitation, ice melting influenced by air temperature and inflow of Arctic Ocean waters (Andrews, J. et al. 2018).

The Greenland Sea has negative trend in ocean mass of -9.10 mm/year and Sea Level Anomaly trend is negative at north of -1 mm/year and positive trend up to 6 mm/year. The positive trend in Sea Level Anomaly close to the Green land is questionable and can be attributed to few data existence during ERS-1 or ERS-2 or Envisat period due to heavy sea ice coverage. Whereas the same area Cryosat-2 provides a narrow strip of SARin data (Anderson OB and Piccini G. 2016). The negative trend in Greenland Sea is influenced by Gravitational attraction of Greenland masses or due to freshwater outflow from the Arctic ocean through western side of Fram Strait (Timmernans and Marshahall., 2020 and Brunnabend S.-E., et al. 2011).

Barents Sea has positive trend in ocean mass of 0.13 mm/year and positive trend in Sea Level Anomaly range from -1 mm/year to 7mm/year. The positive trend here are influenced by the inflow of Atlantic water which are warm, saltier, and denser into the Arctic ocean (Timmernans

and Marshahall., 2020). Kara sea has positive trend in ocean mass of 3.73 mm/year, Laptev sea has positive trend in ocean mass of 6.83 mm/year, East Siberian Sea has a positive trend of 8.25 mm/year and Arctic ocean has positive ocean mass trend of 5.83 mm/year. The positive trends in this region are influenced by the so-called Atlantification of Arctic ocean. The Atlantic water is transferred into Arctic ocean through Fram strait (or may be through Barents Sea) into deep ocean and these are warm and salty water (salty than in arctic water) because of this process if the salt in water increases, the mass of the ocean increases (Polyakov et al., 2020 and Polyakov et al., 2020). The Kara Sea, Laptev Sea and East Siberian Sea all have negative trends range from -2 mm/year to -6 mm/year. This negative trends of Sea Level Anomaly in this region are influenced by the gain of fresh water, net precipitation, run off increased and more discharge from the land to the sea water (Rose, S.K. et al. 2019).

References

[1] Adler, R.F., et al (2003). The Version 2 Global Precipitation Climatology Project (GPCP) Monthly Precipitation Analysis (1979 - Present). J. Hydrometeor., 4(6), 1147-1167.'

[2] Andersen OB and Piccioni G (2016) Recent Arctic Sea Level Variations from Satellites. Front. Mar.Sci.3:76. doi: 10.3389/fmars.2016.00076

[3] Andrews, J, et al. 2018 Climate change and sea ice: Shipping in Hudson Bay, Hudson Strait, and Foxe Basin (1980–2016). Elem Sci Anth, 6: 19. DOI: https://doi.org/10.1525/elementa.281

[4] Brunnabenda, S.-E. et al (2011). Modeled steric and mass-driven sea level change caused by Greenland Ice Sheet melting. Journal of Geodynamics 59– 60 (2012) 219– 225. doi: 10.1016/j.jog.2011.06.001

[5] Cheng, M.K. and J. C. Ries (2017). The unexpected signal in GRACE estimates of C20, J. Geodesy, DOI: 10.1007/s00190-016-0995-5.

[6] Cooley, S. and Landerer, F. (2019). Gravity Recovery and Climate Experiment Follow-on (GRACE-FO) Level-3 Data Product User Handbook. Jet Propulsion Laboratory. California Institute of Technology. Downloaded from: https://podaac-tools.jpl.nasa.gov/drive/files/allData/gracefo/docs/GRACE-FO_L3_Handbook_JPL-D-103133_20200709.pdf

[7] Dobslaw, H., Bergmann-Wolf, I., Dill, R., Poropat, L., Thomas, M., Dahle, C., Esselborn,S., K¨onig, R., Flechtner, F. (2017). A New High-Resolution Model of Non-Tidal Atmosphere and Ocean Mass Variability for De-Aliasing of Satellite Gravity Observations: AOD1B RL06.Geophys. J. Int., 211, 263–269.

[8] Flanders Marine Institute (2018). IHO Sea Areas, version 3. Available online at https://www.marineregions.org/. https://doi.org/10.14284/323

[9] GFZ: https://www.gfz-potsdam.de/en/section/global-geomonitoring-and-gravity-field/projects/gravity-recovery-and-climate-experiment-follow-on-grace-fo-mission/ ,2020. Accessed in November 2020.

[10] GFZ: https://www.gfz-potsdam.de/en/grace/, 2020. Accessed in November 2020.

[11] Kusche, J., Eicker A., and Forootan, E., (2011) "Analyis Tools for GRACE- and Related Data Sets Theoretical Basis", Lecture Notes, Summer school 'Global Hydrological Cycle', Mayschoss, Sept. 12-16, 2011, Bonn University.

[12] Landerer, F. W., Flechtner, F. M., Save, H., Webb, F. H., Bandikova, T., Bertiger, W. I., et al. (2020). Extending the global mass change data record: GRACE Follow-On instrument and science data performance. Geophysical Research Letters, 47, e2020GL088306. https://doi.org/10.1029/2020GL088306.

[13] Peltier, W.R., Argus, D.F. and Drummond, R. (2018) Comment on "An Assessment of the ICE- 6G_C (VM5a) Glacial Isostatic Adjustment Model" by Purcell et al. J. Geophys. Res. Solid Earth, 123, 2019-2018, doi:10.1002/2016JB013844.

[14] Polyakov, I. V., and Coauthors, 2020: Weakening of Cold Halocline Layer Exposes Sea Ice to Oceanic Heat in the Eastern Arctic Ocean. J. Climate, 33, 8107–8123, https://doi.org/10.1175/JCLI-D-19-0976.1.

[15] Rose, S.K.; Andersen, O.B.; Passaro, M.; Ludwigsen, C.A.; Schwatke, C. Arctic Ocean Sea Level Record from the Complete Radar Altimetry Era: 1991‐ 2018. Remote Sens. 2019, 11, 1672. https://www.mdpi.com/2072-4292/11/14/1672

[16] S.-E.Brunnabend, J.Schröter, R.Timmermann ,R.Rietbroek, J.Kusche (2011). Modeled steric and mass-driven sea level change caused by Greenland Ice Sheet melting. Journal of Geodynamics 59–60 (2012) 219–225, doi: 10.1016/j.jog.2011.06.001

[17] Seeber, G. (2003). Satellite Geodesy (2nd Edition). Berlin: Walter de Gruyter.

[18] Shepherd, A. et al (2019). ArticleMass balance of the Greenland Ice Sheet from 1992 to 2018.). https://doi.org/10.1038/s41586-019-1855-

[19] Stewart, R.H. (2000). Introduction to Physical Oceanography. Department of Oceanography, Texas A and M University.

[20] Sun, Y., R. Riva, and P. Ditmar (2016), Optimizing estimates of annual variations and trends in geocenter motion and J2 from a combination of GRACE data and geophysical models, J. Geophys. Res. Solid Earth, 121, doi:10.1002/2016JB013073.

[21] Swenson, S., D. Chambers, and J. Wahr (2008) Estimating geocenter variations from a combination of GRACE and ocean model output, J. Geophys. Res., 113, B08410, doi:10.1029/2007JB005338.

[22] Tapley, et al., (2004). The Gravity Recovery and Climate Experiment: Mission Overview and Early Results. Geophysical Research Letters · May 2004. DOI: 10.1029/2004GL019920

[23] Timmermans, M.-L., & Marshall, J. (2020). Understanding Arctic Ocean circulation: A review of ocean dynamics in a changing climate. Journal of Geophysical Research: Oceans, 125, e2018JC014378. https://doi.org/10.1029/2018JC014378

[24] Uebbing, B., Kusche, J., Rietbroek, R., & Landerer, F. W. (2019). Processing choices affect ocean mass estimates from GRACE. Journal of Geophysical Research: Oceans, 124, 1029–1044. https://doi.org/10.1029/2018JC014341

[25] UTCSR: http://www2.csr.utexas.edu/grace/overview.html, 2020. Accessed in November 2020

[26] Wahr et al (1998). Time variability of the earth's gravity field: hydrological and oceanic effects and their possible detection using GRACE", JGR, Vol. 103, No. B12, p 30,205-30,229, 1998.

[27] Woodgate, R. (2013) Arctic Ocean Circulation: Going Around At the Top Of the World. Nature Education Knowledge 4(8):8. https://www.nature.com/scitable/knowledge/library/arctic-ocean-circulation-going-around-at-the-102811553

[28] Yang, Y. et al. (2020). Summer Changes in Water Mass Characteristics and Vertical Thermohaline Structure in the Eastern Chukchi Sea, 1974–2017

[29] Yi, S. (2019). Application of Satellite Gravimetry to Mass Transports on a Global Scale and the Tibetan Plateau, Springer Theses, https://doi.org/10.1007/978-981-13-7353-4_7

Appendices

Appendix I: Time series of the mean of monthly ocean mass from CSR and GFZ Centres

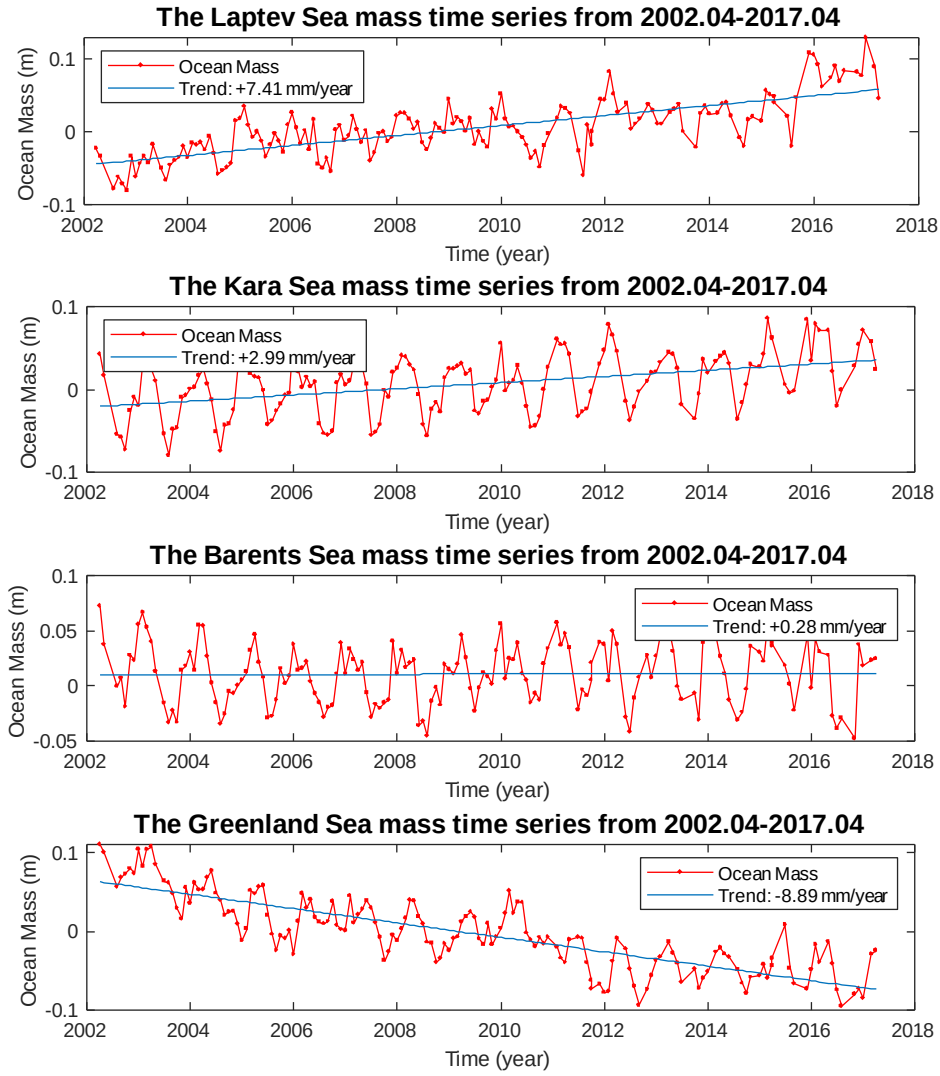

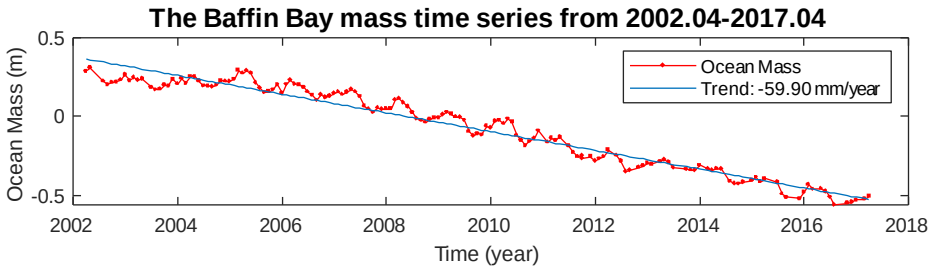
The Baffin Bay mass time series from 2002.04-2017.04
Ocean Mass (m)
Time (year)
Ocean Mass
Trend: -59.90 mm/year

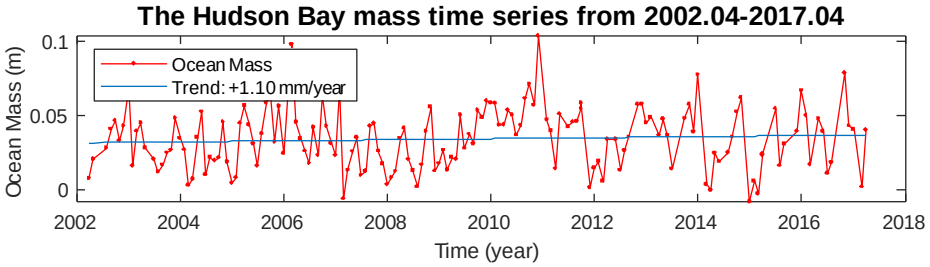
The Hudson Bay mass time series from 2002.04-2017.04
Ocean Mass (m)
Time (year)
Ocean Mass
Trend: +1.10 mm/year

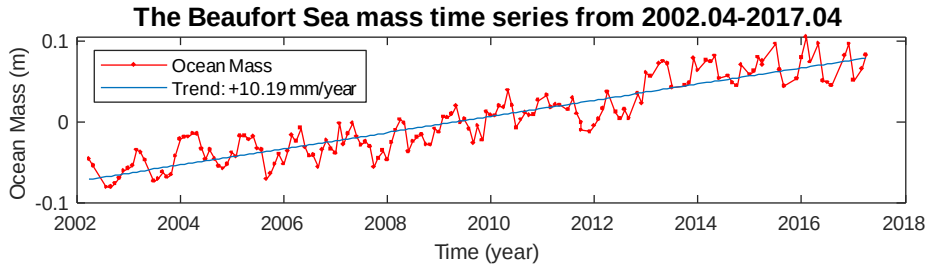
The Beaufort Sea mass time series from 2002.04-2017.04
Ocean Mass (m)
Time (year)
Ocean Mass
Trend: +10.19 mm/year

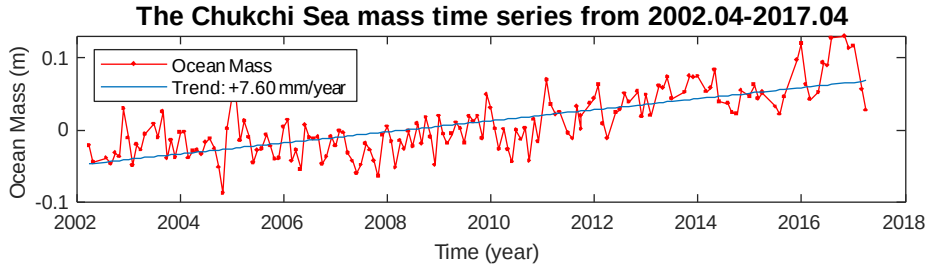
The Chukchi Sea mass time series from 2002.04-2017.04
Ocean Mass (m)
Time (year)
Ocean Mass
Trend: +7.60 mm/year

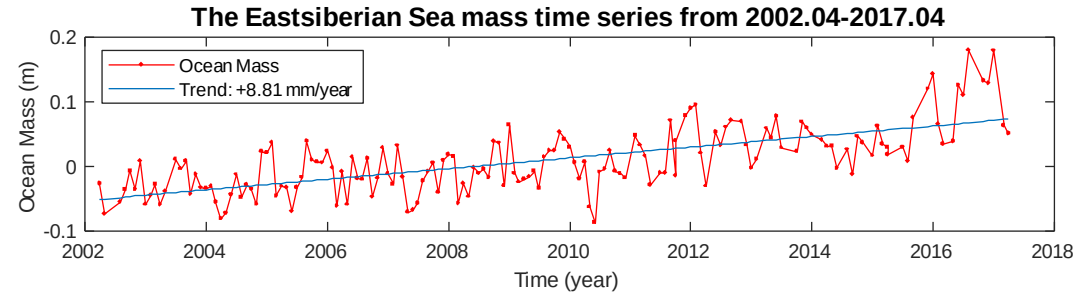

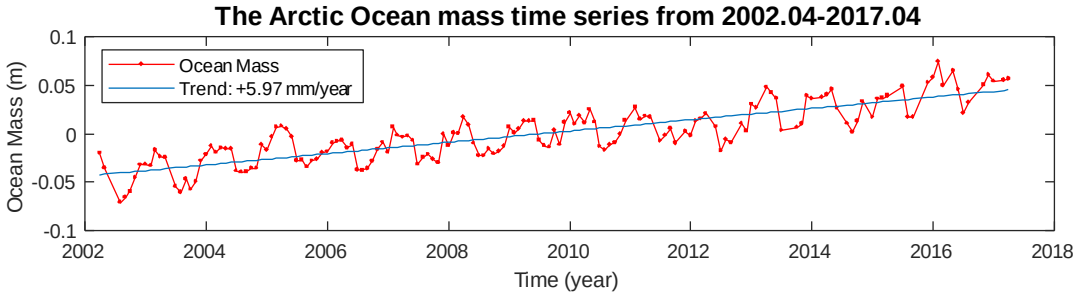

APPENDIX II: Case 01 the C_{20} replaced and the degree 01 added for both GFZ and CSR

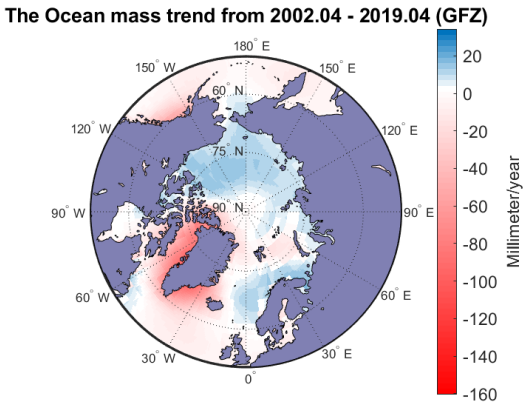

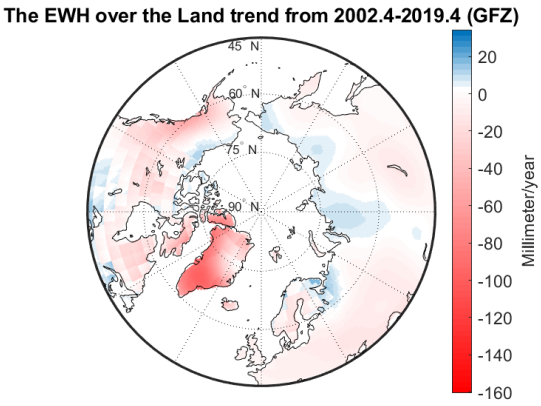

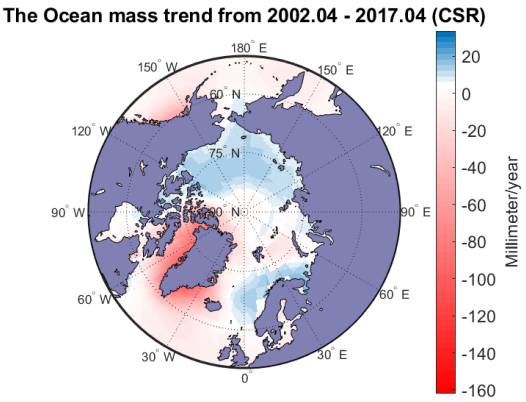

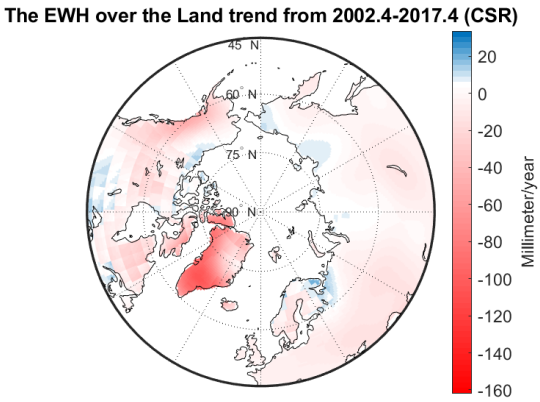

APPENDIX III: Case 02 the C_{20} NOT replaced and the degree 01 added for both GFZ and CSR

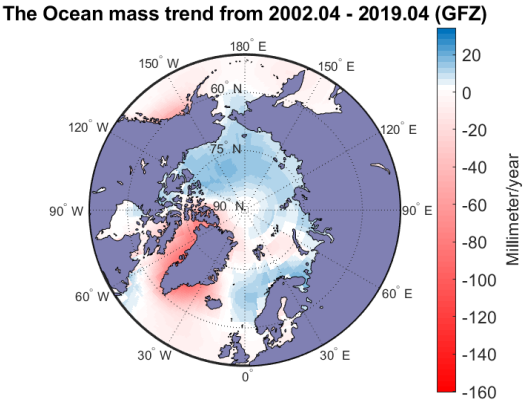

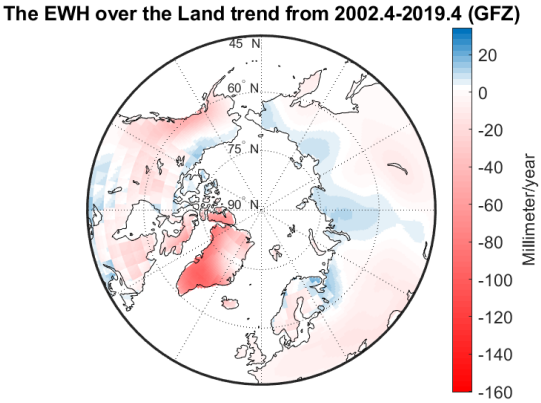

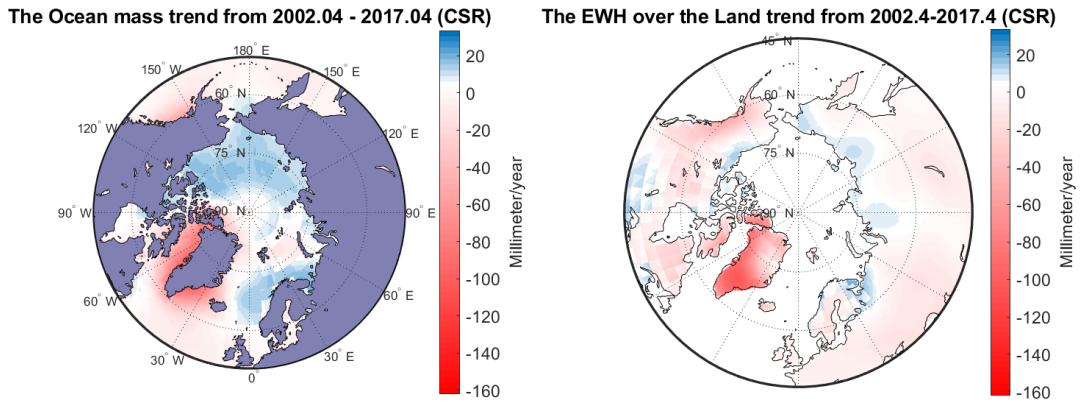

APPENDIX IV: Case 03 the C_{20} NOT replaced and the degree 01 NOT added for both GFZ and CSR

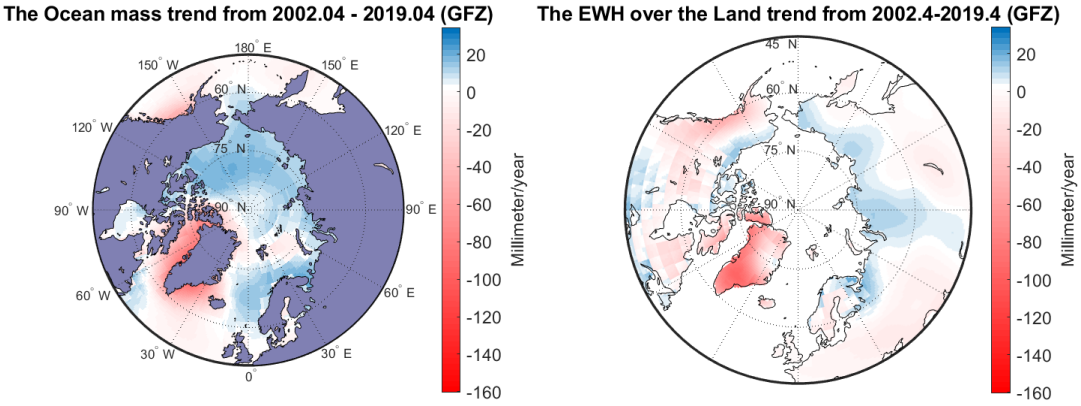

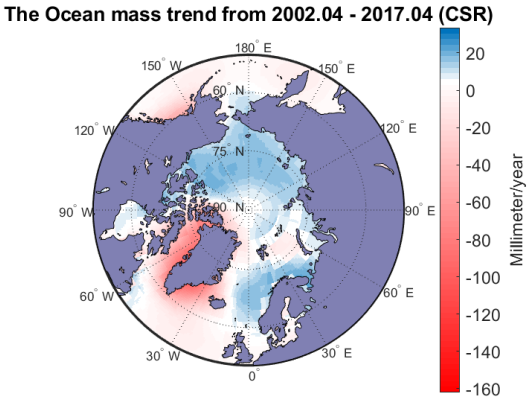

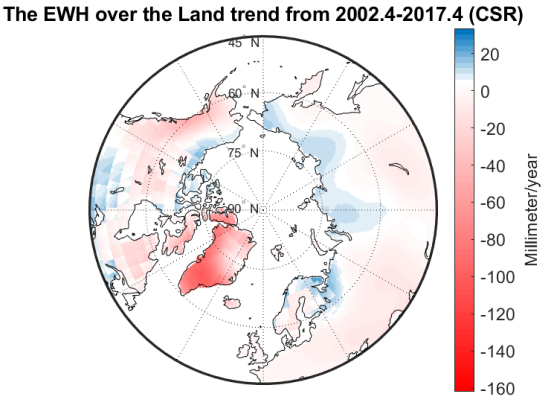

APPENDIX V: Case 04 the C_{20} replaced and the degree 01 NOT added for both GFZ and CSR

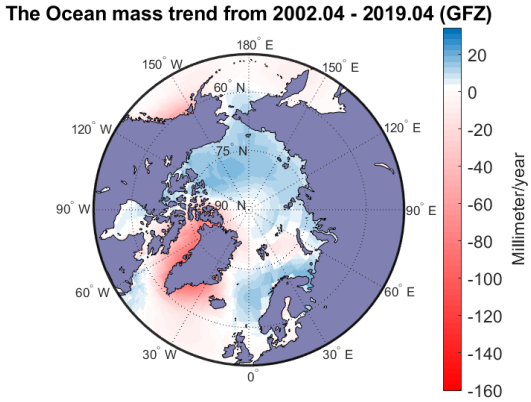

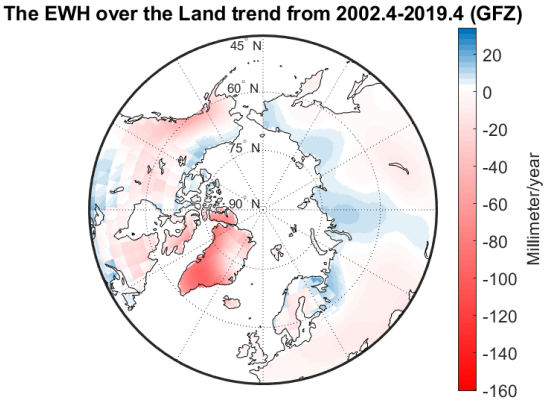

The Ocean mass trend from 2002.04 - 2017.04 (CSR)

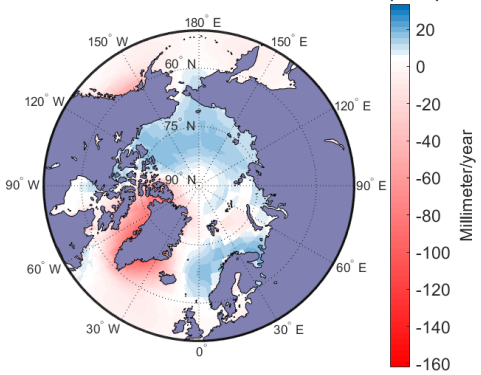

The EWH over the Land trend from 2002.4-2017.4 (CSR)